INVESTIGATION INTO DYNAMIC RESPONSE OF THE ARM OF THE RADIAL DRILLING MACHINE RD 6

A THESIS

Submitted in Partial Fulfilment of the Requirments

For the Degree of

MASTER OF TECHNOLOGY

by

JUTURI RADHAKRISHNA MOORTHY

to the

DEPARTMENT OF MECHANICAL ENGINEERING

INDIAN INSTITUTE OF TECHNOLOGY, KANPUR

SEPTEMBER, 1971

ACKNOWLEDGEMENT

The author wishes to express his gratitude to Dr. [illegible] Kainth of the department of Mechanical Engineering for his keen interest shown in this work and for his invaluable suggestions which helped a lot for the completion of the work. Sincere thanks are due to Dr. R.G.R. Iyengar of the Department of Aeronautical Engineering for his valuable suggestions at different stages of the work. Thanks are also due to Messers Hindustan Machine Tools Limited, Bangalore for kindly supplying the necessary design details of the arm of the radial drilling machine RD 6.

Juturi Radhakrishna Moorthy

CERTIFICATE

Certified that this work has been carried out under my supervision and that this has not been submitted elsewhere for a degree.

(G.S. Kainth)
Assistant Professor
Department of Mechanical Engg.

SYNOPSIS

of the

Dissertation on

INVESTIGATION INTO DYNAMIC RESPONSE OF
THE ARM OF THE RADIAL DRILLING MACHINE RD 6
A Thesis Submitted
In Partial Fulfillment of the Requirements
for the Degree of
MASTER OF TECHNOLOGY
in
Mechanical Engineering
by

JUTURI RAMAKRISHNA MOORTHY
to the
Department of Mechanical Engineering
INDIAN INSTITUTE OF TECHNOLOGY, KANPUR

September, 1971

During machining on a machine tool, the maximum rate of metal removal is limited by a set of vibrating forces acting on the machine tool structure and the response of the machine tool structure to these vibrating forces. The response of a machine tool structure to a set of harmonic exciting forces can be found out from the modes of vibration.

In the present work, lumped-mass technique is applied to predict the static deflection, the natural frequencies and modes of vibration, and the dynamic response of the arm of the radial drilling machine RD 213 to harmonic excitations for two alternative designs of the arm. From the investigation it is concluded that the arm has nearly identical static and dynamic responses for the original and the alternative designs.

NOMENCLATURE

A	Cross sectional area of arm-element
$[A]$	Rectangular matrix relating elemental mass matrices to combined mass matrix
$[C]$	Damping matrix
E	Young's modulus of material of the arm
E_j	j-th element in the mathematical model of the arm
$\{F_s\}_j$	Vector of generalised forces on j-th element
G	Rigidity modulus of material of the arm
$[I]$	Identity matrix
I_y	Principal second moment of area about y_s axis
I_z	Principal second moment of area about z_s axis
I_{yz}	Product moment of area in local coordinates
$I_{mxx}, I_{myy}, I_{mzz}$	Mass moment of inertia of half arm-element about the respective axes
i, j	Suffixes
k	Superfix
$[K]$	Assembled stiffness matrix
$[k]_j$	Stiffness matrix of j-th arm-element in local coordinates
$[\bar{K}]_j$	Stiffness matrix of j-th arm-element in datum coordinates.
$\bar{K}_{Aj}$	Sub-matrix of the elemental stiffness matrix of j-th element in datum coordinates
L	Length of element

l_{ox}, l_{oy}, l_{oz}	Direction cosines
$[M]$	Combined mass matrix of the arm
m_i	Mass of half element of the arm
$[m]_j$	Mass matrix of j-th element in local coordinates
$[\bar{m}_j]$	Mass matrix of j-th element in datum coordinates
$\bar{m}_{ij}$	Submatrix of elemental mass matrix in datum coordinates
m_{ox}, m_{oy}, m_{oz}	Direction cosines
$[N]$	A matrix equal to $[M]^{1/2}$
n	Number of degrees of freedom on arm-element
n_{ox}, n_{oy}, n_{oz}	Direction cosines
$\{P\}$	Vector of external loading on the arm
$[R]$	A unitary matrix
S_x	First moment of area about x axis
S_y	First moment of area about y axis
$\{U\}$	Vector of displacements on the assembled structure in datum coordinates
$\{u\}$, $\{\bar{u}\}$	Vector of elemental displacements in local and datum coordinates respectively
$\{\ddot{\bar{u}}\}$	Double derivative with respect to time of $\{\bar{u}\}$
ω	Frequency
ω_n	Natural frequency
(XYZ)	Datum coordinate system
(xyz)	Local coordinate system for arm-element
$(x_p\ y_p\ z_p)$	Principal coordinate system for arm-element
$\{X\}$, $\{Y\}$, $\{Z\}$	Vectors of amplitudes of displacements
$\{x\}$, $\{y\}$, $\{z\}$	Displacement vectors

x_{ca}, y_{ca}	Coordinates of centre of sectional area
δ	An increment in a value
ξ	Damping coefficient
θ	Angle between x and x_p axes
θ_{Xx}	Angle between X and x axes
Λ	3 x 3 matrix of direction cosines of local coordinates relative to datum coordinates
$[\lambda]$	n x n matrix of direction cosines
ρ	Density

LIST OF FIGURES

Page

Page

CONTENTS

CHAPTER I

INTRODUCTION

The machining of metals is often accompanied by violent relative vibrations between workpiece and cutting tool which is known as chatter. Chatter is undesirable in machine tools since it affects dimensional accuracy and causes undulations on the machined surface giving poor finish.

Dynamic Stability of Machine Tools:

A chatter free machine tool is said to be in steady state. If a machine tool in steady state is disturbed, for example when the cutting tool strikes a hard spot in the workpiece material, an increment dF in the steady cutting thrust force F is caused. This increment dF causes a deflection in the machine tool structure. When the machine tool structure is released of the incremental cutting thrust force, the machine tool is thrown into vibration which is superimposed on the steady state motion. The machine tool is said to be dynamically stable if the vibrations die down and steady state is established in the machine tool with time. On the other hand, the machine tool is said to be dynamically unstable, if the vibrations build up with time.

Causes Affecting Stability of Machine Tools:

The incremental cutting thrust force dF depends not only on the displacement brought about by the disturbance of the steady state, but also on the velocity of the disturbance. Velocity dependent forces may be called as damping forces. Hence, the introduction of the incremental cutting force dF affects the damping forces present in the machine-tool system. The damping present in the system is increased, thereby decaying the vibrations, if the damping introduced into the system is positive[14]. On the other hand, the overall damping present in the system may become negative, thereby building up the vibrations, if the damping introduced into the system is highly negative. In the latter case, the energy needed for building up the vibrations is taken from the machine-tool drive which acts as a source of energy.

Stability Chart:

A graphical representation of maximum width of cut against cutting speed corresponding to the onsetting of chatter in a machine tool is known as stability chart. It is essential to know the dynamic response of the structure of a machine tool to predict[9] its stability.

Response Locus:

The dynamic response of a machine tool is represented in the form of harmonic response locus. Harmonic response locus

is a graph in which the in-phase and the out-of-phase components of displacement of a structure to an exciting harmonic force are plotted along two axes perpendicular to each other, the frequencies being marked along the length of the curve.

The experimental techniques available to predict the harmonic response locus of a machine tool are time consuming and expensive. Also, with the present day needs for larger capacity machine tools, optimization of their structures at the design stage itself is essential. It is difficult to achieve this by experimental techniques.

Literature Survey:

Investigations into machine tool dynamics applying lumped parameter techniques were carried out by Tobias, Taylor, Cowley, Fishwick and Fawcett[1,2,3,4,8].

Taylor and Tobias[1,4] developed lumped parameter technique for application to machine tool structures. Taylor[2,3] applied the lumped-mass technique to predict mode shapes and frequencies of vibration, and response to harmonic excitations for the case of a lathe model and three versions of a horizontal milling machine. Taylor conducted experiments on perspex model of a lathe and observed 'good agreement' between computed and experimental results. He concluded that lumped parameter technique is a 'powerful and economical tool' for optimizing machine tool structures.

Lumped-mass techniques are used by Cowley and Fawcett[8] also for computing the static flexibilities, and natural frequencies and modes of vibration of various machine tool structures, e.g. planomilling machine structure.

In the present work, lumped parameter technique is used to predict the dynamic response of the arm of the radial drilling machine RD 6 from design drawings. The technique is applied to predict the dynamic response of the arm to harmonic excitations for two alternative designs of the arm of the radial drilling machine.

CHAPTER II

INERTIA AND STIFFNESS PROPERTIES OF STRUCTURES

2.1 General:

Machine tools are vibratory systems having distributed mass and elasticity. All continuous systems i.e. systems having distributed mass and inertia have infinite degrees-of-freedom. Vibration theory is not yet fully developed to tackle continuous systems with complicated sections and so, they are usually approximated by a system with finite degrees-of-freedom. There are two mathematical models which satisfactorily represent[5] continuous systems. They are given by,

a) Lumped-mass model, and

b) Distributed-mass model.

Lumped-mass representation is the simpler of the two mathematical models as far as the inertia properties of the structural elements are considered. In this idealization, lumped masses are placed at station points and elements connecting the masses are supposed to be elastic and massless.

Though the lumped-mass technique is not as accurate as the distributed-mass technique[5], it is usually preferred because of the computational advantages resulting from the diagonal mass matrix in lumped-mass technique.

The basic steps in the lumped parameter technique are as follows:

1. Idealization of the actual continuous structure to make the lumped-mass model by selecting station points where masses are lumped.

2. Selection of the local and the datum coordinate systems (x,y,z) and (X,Y,Z) respectively.

3. Calculation of elemental mass matrix in the local coordinate system.

4. Determination of matrix of direction cosines for each element.

5. Calculation of elemental mass matrix in datum coordinate system.

6. Calculation of elemental stiffness matrix in local and datum coordinates.

7. Combination of elemental mass matrices in datum coordinates to form the mass matrix for the complete structure and eliminate rows and columns corresponding to rigid-body degrees-of-freedom to establish reduced mass matrix.

8. Combination of elemental stiffness matrices in datum coordinates to form the stiffness matrix for the complete structure and eliminate rows and columns corresponding to rigid-body degrees-of-freedom.

9. Calculation of dynamic matrix and evaluate natural frequencies and modes of vibration of the radial drill-arm.

10. Finding out of the dynamic response of the radial drill-arm for given harmonic excitations.

The foregoing basic steps are elaborated in the following sections.

2.2 <u>Idealisation of the Structure of the Arm:</u>

The structural details of the radial drill-arm are shown in Figures 1, 2, 3, 4, 5 and 6. Fig. 1 shows the plan view for the original design, Fig. 2 shows the elevations from front and back for the original design, Fig. 3 shows the section CC in Fig. 1.(this is common for the original and the alternative designs), Fig. 4 shows the section BB for the original design, Fig. 5 shows the section of the element E_7 for the alternative design and Fig. 6 shows the section AA for the original design (See Fig. 1).

Fig. 7 shows the mathematical model of the arm. The arm is eccentrically fitted on the vertical column of the radial drill. A station point is located wherever there is a drastic change in the cross section of the arm along its length. In all, fourteen station points are located and the arm-elements are marked E_1 to E_{13}. The station points are numbered in the fashion shown in Fig. 7 so as to ensure a banded assembled stiffness matrix. A matrix is said to be banded if all the elements lying further than a certain distance from the leading diagonal are zeros.

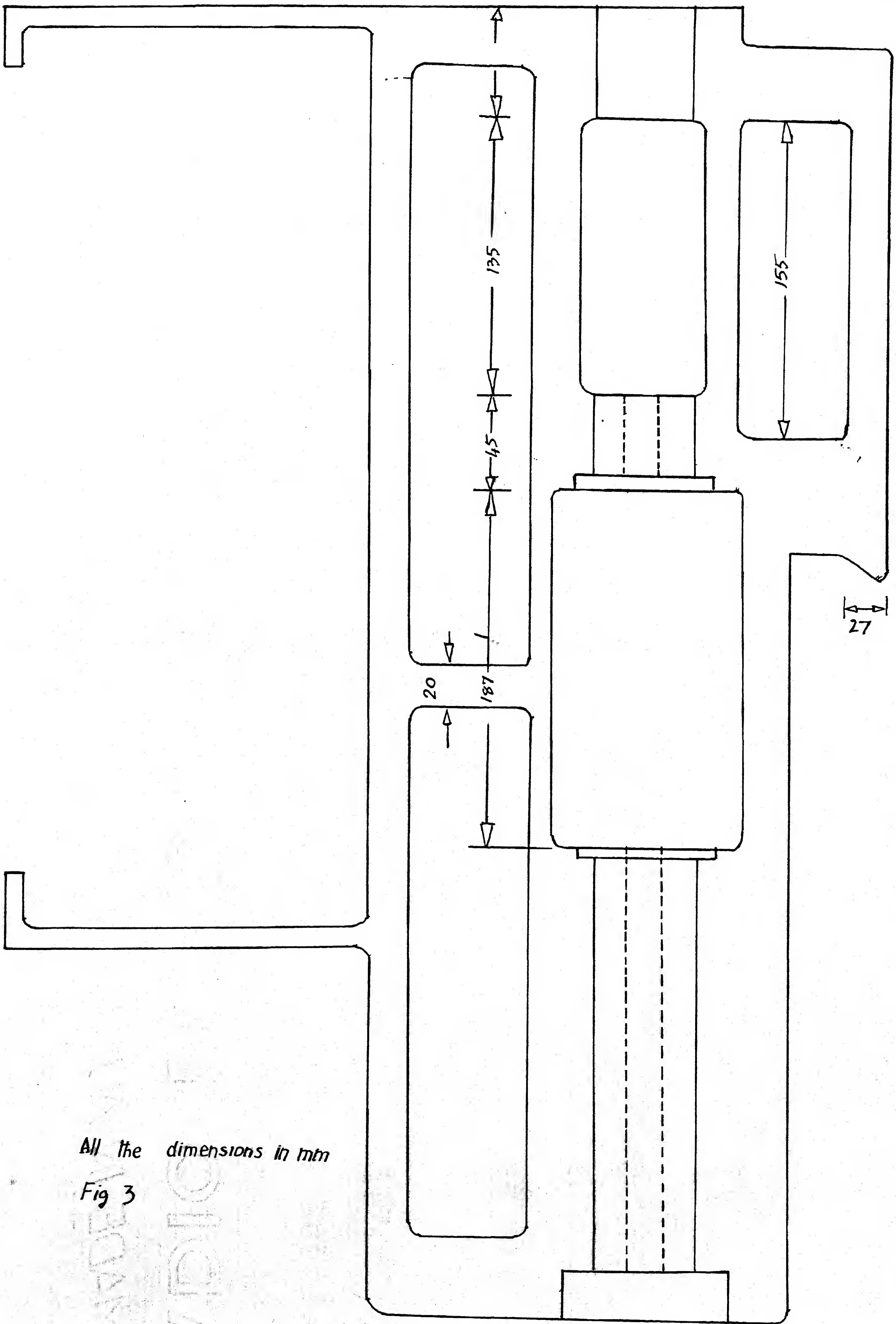

All the dimensions in mm

Fig 3

details of SECTION CC

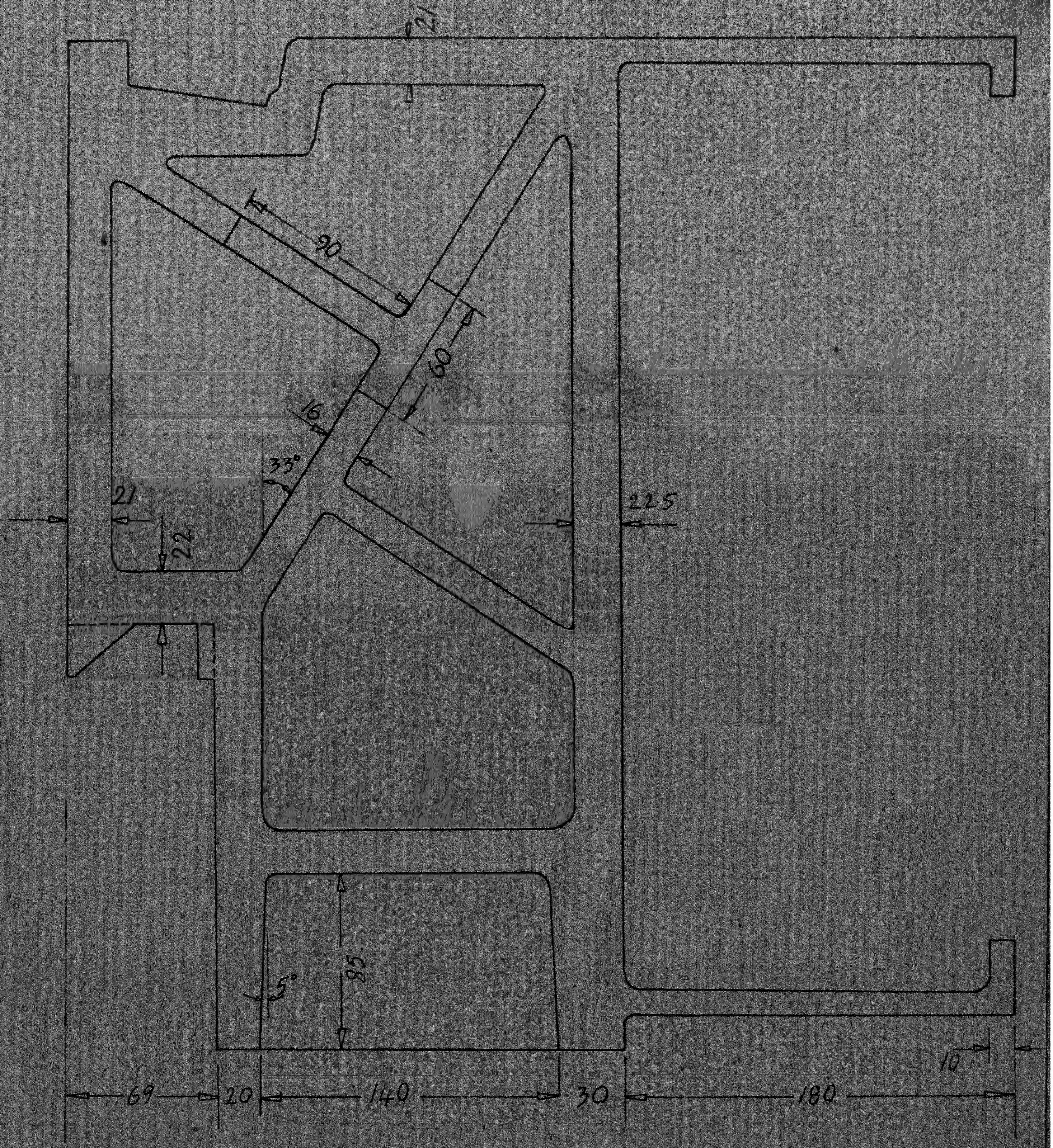

Details of the Arm at

SECTION BB

Original Design

Fig. 4

All dimensions in mm

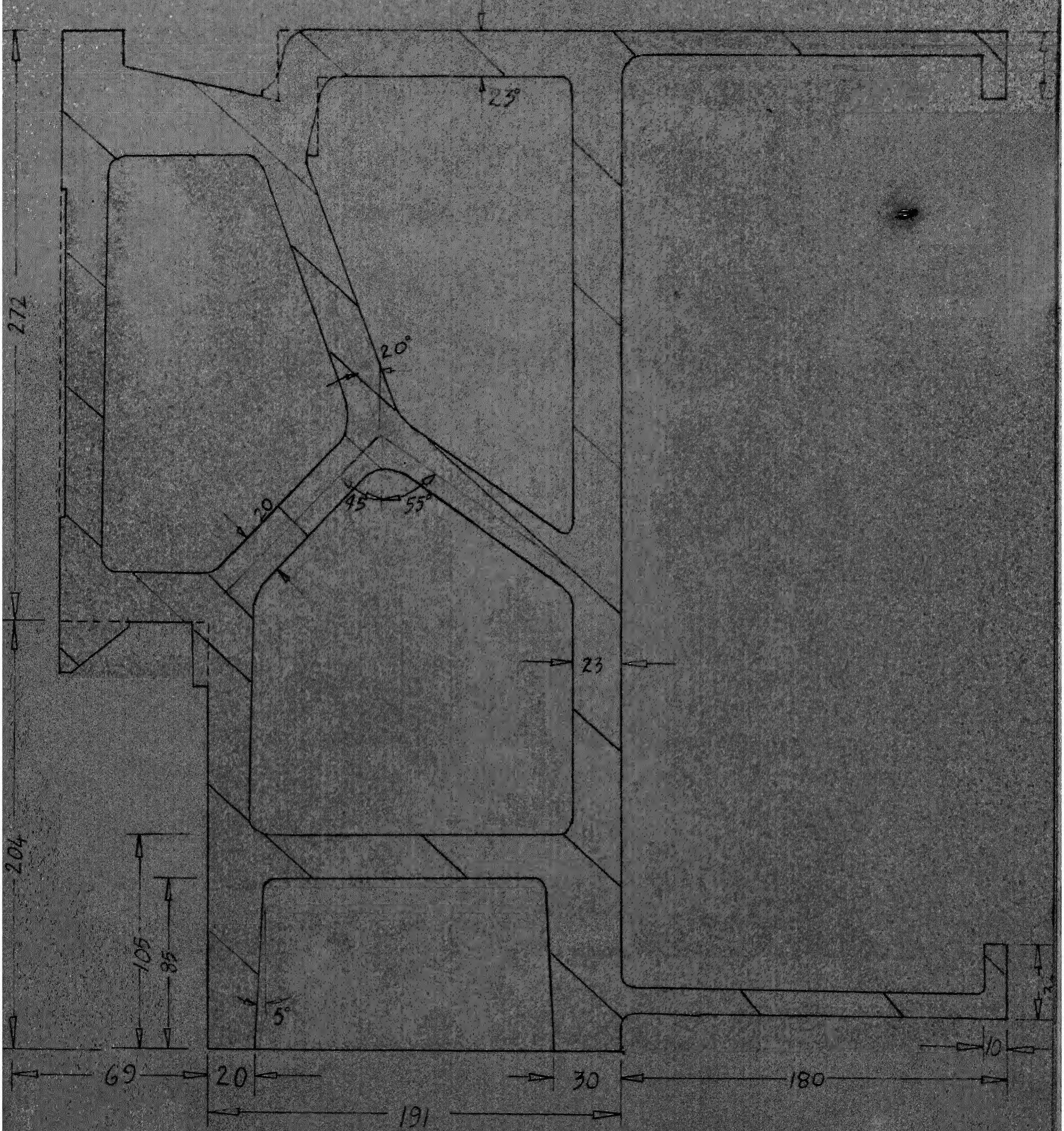

details of SECTION E7
Alternative Design
All dimensions in mm
Fig.5

Details of SECTION AA
Original Design
All the dimensions in mm

Fig 6

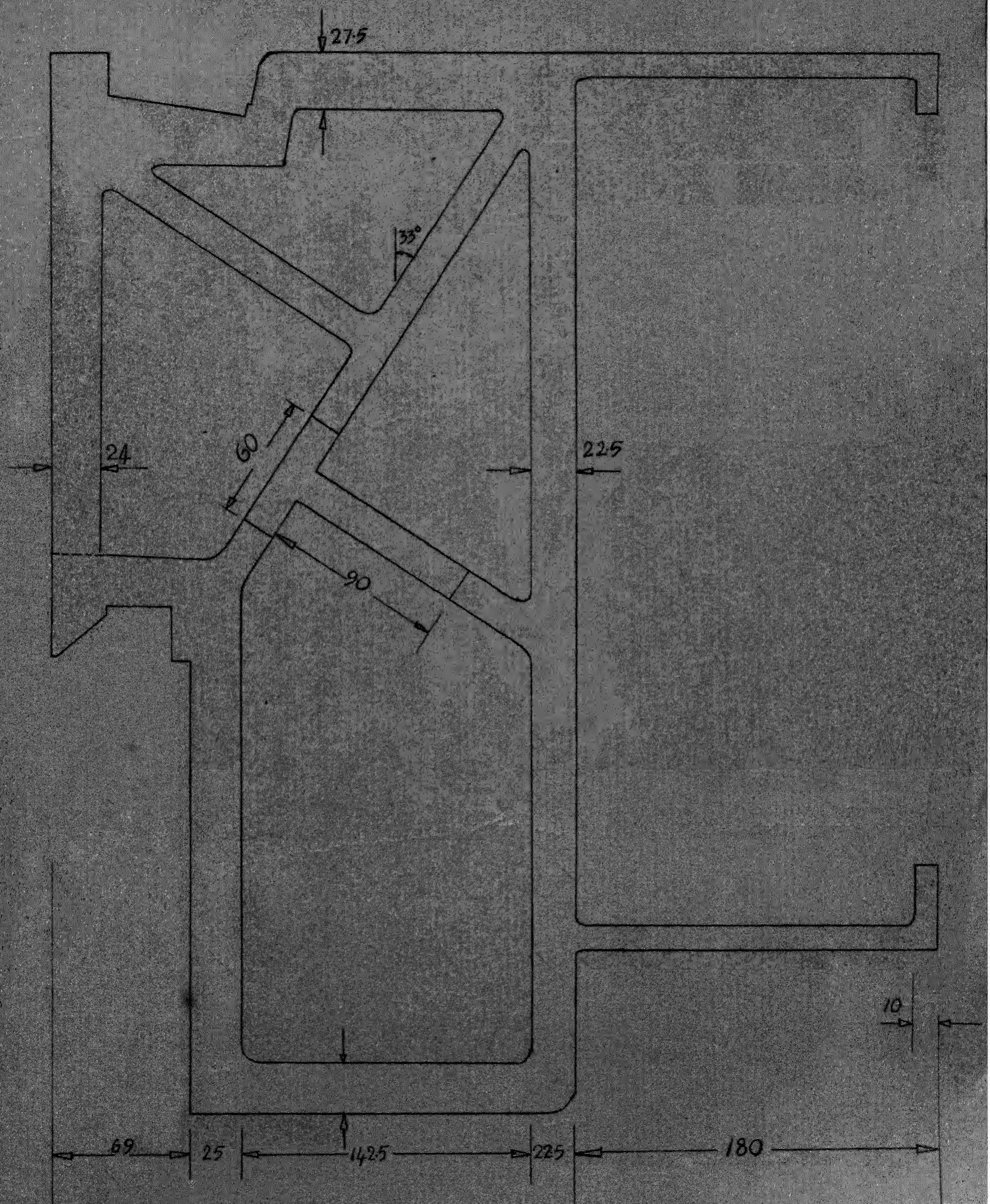

Mathematical Model of Radial Drilling Machine - Arm

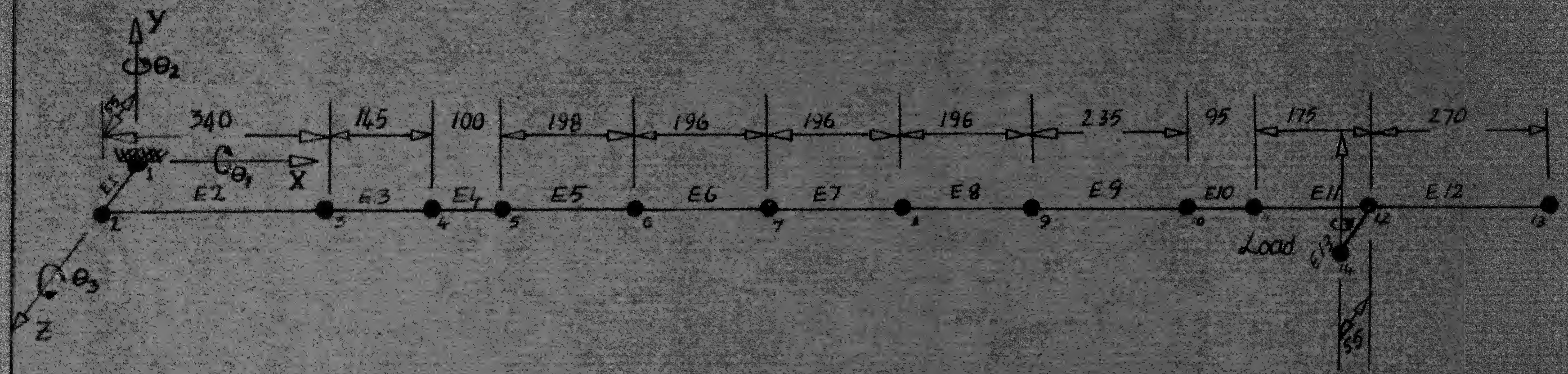

STATION POINT	VARIABLES	STATION POINT	VARIABLES	STATION POINT	VARIABLES
1	$U_1 - U_6$	6	$U_{31} - U_{36}$	11	$U_{61} - U_{66}$
2	$U_7 - U_{12}$	7	$U_{37} - U_{42}$	12	$U_{67} - U_{72}$
3	$U_{13} - U_{18}$	8	$U_{43} - U_{48}$	13	$U_{73} - U_{78}$
4	$U_{19} - U_{24}$	9	$U_{49} - U_{54}$	14	$U_{79} - U_{84}$
5	$U_{25} - U_{30}$	10	$U_{55} - U_{60}$		

Station Point 1 is rigidly fixed.
At each of the other stationary Points 3 translatory and 3 rotational displacements exist.

Fig 7

The arm is considered to be rigidly fixed along the axis of the vertical column of the radial drill (this position corresponds to station point 1 in the mathematical model). The effect of vibrations of the vertical column itself on the arm during machining are not considered since the problem is concerned with optimizing the design of ribbing in the arm only.

Most of the actual structural details of the arm are taken into consideration. A few details are slightly altered and a few other minor details are ignored for simplifying the structure for computational convenience.

The sectional details of the saddle represented by the element E_{13} in Fig. 7 are not available. The sectional details of the element E_2 are used for the element E_{13}, the saddle being heavy and stiff like the element E_1 (The element E_1 has the largest sectional properties of all the elements of the arm). The element E_1 is fictitious and is the shortest of all the elements of the arm. The element E_1 is also considered to have the same sectional properties as the element E_2, E_1 being situated just before E_2.

Each element is considered to have uniform cross section along its length. Even though the elements E_3 to E_{12} are uniformly tapering, however, the cross sectional details for these elements are taken at the centre of each element representing uniform cross section, supposing equivalence.

All the geometrical characteristics viz. elemental lengths and sectional details are taken from the design drawings.

At each station point, six displacements - three translational and three rotational-are considered. There are altogether 84 displacements on the arm. Out of these 84 displacements, the six displacements corresponding to the rigid-body boundary conditions are eliminated by making them zero, thus reducing the total number of displacements (degrees-of-freedom) on the structure to 78.

2.3 Elemental Mass Matrix in Local and Datum Coordinates:

The mass matrix of each arm-element is calculated from area of cross section, length, and density of that particular element under consideration. The mass matrix for the unassembled element is calculated in local coordinates and is transformed into datum coordinates by a suitable transformation. Since the model is a lumped-mass one, the elemental mass matrix is diagonal and is given by,

$$[m] = \left\lceil m_1 \; m_1 \; m_1 \; I_{mxx} \; I_{myy} \; I_{mzz} \right\rfloor \qquad (2.3.1)$$

where m_1 is the mass and I_{mxx}, I_{myy} and I_{mzz} are the mass moments of inertia of half the element about the specified axes. Expressions for the elemental masses and moments of inertia are derived in Appendix II.

The mass matrix in the local coordinate system is transformed into the datum coordinate system (X,Y,Z) (See Fig. 7) which is common to all the elements of the arm. This is done so

that all the displacements of discrete elements can be conveniently studied by a single datum. The origin of this datum system is located at the point where the radial drill-arm is considered to be rigidly fixed.

The matrix relating the displacements in the local coordinates to those in the datum system is given by[19]

$$\{u\} = [\lambda]\{\bar{u}\} \qquad (2.3.2)$$

where $\{u\}$ and $\{\bar{u}\}$ are vectors of elemental displacements in the local and datum coordinates respectively and $[\lambda]$ is a n x n matrix, n being the degrees of freedom on the element.

$[\lambda]$ is given by

$$[\lambda] = \begin{bmatrix} \Lambda & 0 & 0 & 0 \\ 0 & \Lambda & 0 & 0 \\ 0 & 0 & \Lambda & 0 \\ 0 & 0 & 0 & \Lambda \end{bmatrix} \qquad (2.3.3)$$

where,

$$\Lambda = \begin{bmatrix} l_{ox} & m_{ox} & n_{ox} \\ l_{oy} & m_{oy} & n_{oy} \\ l_{oz} & m_{oz} & n_{oz} \end{bmatrix} = \begin{bmatrix} \cos\theta_{Xx} & \cos\theta_{Yx} & \cos\theta_{Zx} \\ \cos\theta_{Xy} & \cos\theta_{Yy} & \cos\theta_{Zy} \\ \cos\theta_{Xz} & \cos\theta_{Yz} & \cos\theta_{Zz} \end{bmatrix} \qquad (2.3.4)$$

and represents a matrix of direction cosines of local coordinates ox, oy and oz relative to the datum coordinates OX, OY, and OZ. The angle between X and x axes is denoted by θ_{Xx} in Eqn.(2.3.4). For the elements E_2 to E_{12}, Λ is given by,

$$\Lambda = \begin{bmatrix} 1 & 0 & 0 \\ 0 & \cos\theta & -\sin\theta \\ 0 & \sin\theta & \cos\theta \end{bmatrix} \qquad (2.3.5)$$

and for the elements E_1 and E_{13} it is given by,

$$\Lambda = \begin{bmatrix} 0 & 0 & 1 \\ \sin\theta & \cos\theta & 0 \\ -\cos\theta & \sin\theta & 0 \end{bmatrix} \qquad (2.3.6)$$

The elemental mass matrix in datum coordinates is given by[19]

$$[\bar{M}] = [\lambda]^T [m][\lambda] \qquad (2.3.7)$$

By substitution for $[\lambda]$ from Eqn. (2.3.3) into Eqn.(2.3.7), the elemental mass matrix in datum coordinates for the elements E_2 to E_{12} takes the form,

$$[\bar{M}] = \lceil (m_1)(m_1)(m_1)(I_{mxx})(I_{myy}\cos^2\theta + I_{mzz}\sin^2\theta)$$
$$(I_{myy}\sin^2\theta + I_{mzz}\cos^2\theta)\,(m_1)(m_1)(m_1)(I_{mxx})$$
$$(I_{myy}\cos^2\theta + I_{mzz}\sin^2\theta)(I_{myy}\sin^2\theta + I_{mzz}\cos^2\theta)\rfloor \,.$$

$$(2.3.8)$$

and for the elements E_1 and E_{13}, Eqn. (2.3.7) takes the form,

$$[\bar{M}] = \lceil (m_1)(m_1)(m_1)(I_{myy}\sin^2\theta + I_{mzz}\cos^2\theta)$$
$$(I_{myy}\cos^2\theta + I_{mzz}\sin^2\theta)(I_{mxx})(m_1)(m_1)(m_1)$$
$$(I_{myy}\sin^2\theta + I_{mzz}\cos^2\theta)(I_{myy}\cos^2\theta + I_{mzz}\sin^2\theta)$$
$$(I_{mxx})\rfloor \qquad (2.3.9)$$

The diagonal matrices given in the foregoing Eqns. (2.3.8) and (2.3.9) are actually non-diagonal with two non-zero off-diagonal elements. These two off-diagonal elements are a product of ($I_{myy} - I_{mzz}$) and sin 2θ. As each term of the above product is small in comparison to the other elements of the matrix, their product will be small. So, the two non-diagonal elements are neglected considering the advantages resulting from diagonal mass matrices.

For computational convenience, each $\bar{M}$ is partitioned into four sub-matrices of order 6 x 6 as given by,

$$\bar{M}_j = \begin{matrix} \bar{M}_{Aj} & \bar{M}_{Bj} \\ \bar{M}_{Cj} & \bar{M}_{Dj} \end{matrix} \qquad (2.3.10)$$

where the subscript j refers to the element number.

2.4 Elemental Stiffness Matrix in the Local and the Datum Coordinates:

A typical beam element, along with the location and direction of forces, is shown in Fig. 8. The element is considered to be capable of resisting axial forces F_1 and F_7, bending moments F_5, F_6, F_{11} and F_{12} about the two axes in the plane of its cross section, shear forces F_2, F_3, F_8 and F_9 and twisting moments F_4 and F_{10}. The corresponding displacements u_1 to u_{12} are taken positive in the positive directions of forces.

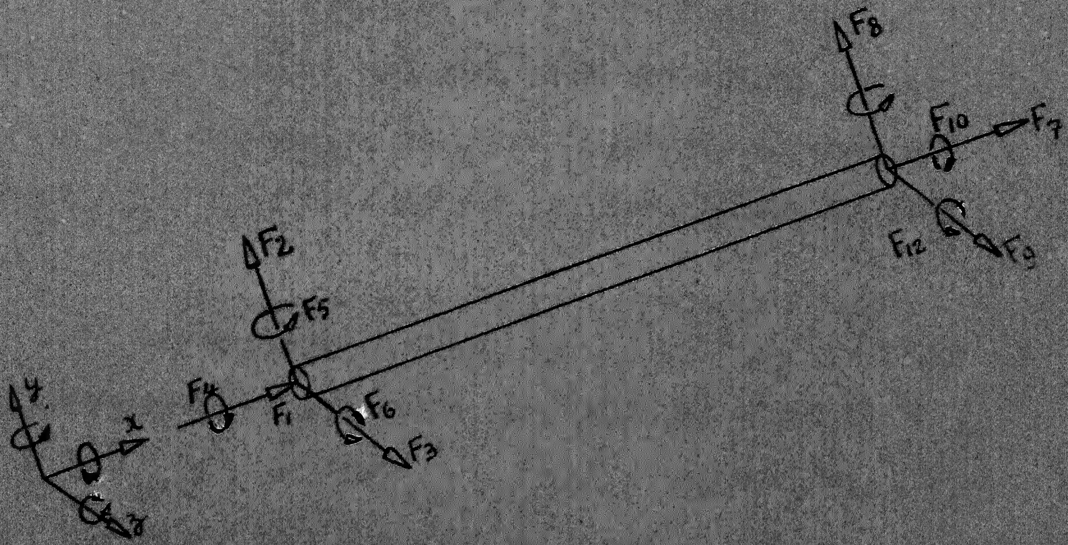

A typical beam element along with the direction and location of forces

Fig. 8

Since 12 independent forces are acting on the beam element, the elemental stiffness matrix is of order 12 x 12. The stiffness matrix can be derived[19] by obtaining solutions of differential equations for the elemental displacements.

The 12 x 12 elemental stiffness matrix can be constructed by 2 x 2 and 4 x 4 sub-matrices if the local axes of the cross section are chosen to coincide with the corresponding principal axes -x axis coinciding with the longitudinal axis of the beam element. The stiffness matrix is given by the Expression[19] (2.4.1).

In the Expression (2.4.1), ϕ_y and ϕ_z are known as shear deformation parameters and they are equal to[19] $12E\, I_z/(GA_{sy}\, L^2)$ and $12E\, I_y/(GA_{sz}\, L^2)$ respectively, I_y and I_z being the second moments of area about the principal axes in the plane of cross section of the beam element, E being the Young's modulus and G being the rigidity modulus. Since the arm under consideration is non-slender, these shear deformation parameters are taken into consideration making the first approximation that $A_{sy} = A_{sz} = A$.

The relationship between elemental forces and elemental displacements is given by,

$$\{F\} = [k]\ \{u\} \qquad (2.4.2)$$

Stiffness Matrix in Datum Coordinates:

The elemental stiffness matrix $\overline{K}$ in datum coordinates is given by[19],

$$
\begin{bmatrix}
\frac{EA}{L} \\
0 & \frac{12EI_z}{L^3(1+\phi_y)} \\
0 & 0 & \frac{12EI_y}{L^3(1+\phi_z)} \\
0 & 0 & 0 & \frac{GJ}{L} \\
0 & 0 & \frac{-6EI_y}{L^2(1+\phi_z)} & 0 & \frac{(4+\phi_y)EI_y}{L(1+\phi_z)} \\
0 & \frac{6EI_z}{L^2(1+\phi_y)} & 0 & 0 & 0 & \frac{(4+\phi_y)EI_z}{L(1+\phi_y)} & & & & \text{Symmetric} \\
-\frac{EA}{L} & 0 & 0 & 0 & 0 & 0 & \frac{EA}{L} \\
0 & \frac{-12EI_z}{L^3(1+\phi_y)} & 0 & 0 & 0 & \frac{-6EI_z}{L^2(1+\phi_y)} & 0 & \frac{12EI_z}{L^3(1+\phi_y)} \\
0 & 0 & \frac{-12EI_y}{L^3(1+\phi_z)} & 0 & \frac{6EI_y}{L^2(1+\phi_z)} & 0 & 0 & 0 & \frac{12EI_y}{L^3(1+\phi_z)} \\
0 & 0 & 0 & -\frac{GJ}{L} & 0 & 0 & 0 & 0 & 0 & \frac{GJ}{L} \\
0 & 0 & \frac{-6EI_y}{L^2(1+\phi_z)} & 0 & \frac{(2-\phi_z)EI_y}{L(1+\phi_z)} & 0 & 0 & 0 & \frac{6EI_y}{L^2(1+\phi_z)} & 0 & \frac{(4+\phi_z)EI_y}{L(1+\phi_z)} \\
0 & \frac{6EI_z}{L^2(1+\phi_y)} & 0 & 0 & 0 & \frac{(2-\phi_y)EI_z}{L(1+\phi_y)} & 0 & \frac{-6EI_z}{L^2(1+\phi_y)} & 0 & 0 & 0 & \frac{(4+\phi_y)EI_z}{L(1+\phi_y)}
\end{bmatrix}
\qquad (2.4.1)
$$

$$[\bar{K}] = [\lambda]^T [k][\lambda] \qquad (2.4.3)$$

where $[\lambda]$ is the same transformation matrix as given in Eqn. (2.3.2).

For computational convenience, each matrix like $[\bar{K}]$ is partitioned into four 6 x 6 sub-matrices as given by,

$$[\bar{K}_j] = \begin{bmatrix} \bar{K}_{Aj} & \bar{K}_{Bj} \\ \bar{K}_{Cj} & \bar{K}_{Dj} \end{bmatrix} \qquad (2.4.4)$$

where the subscript j stands for element number.

2.5 Combined Mass Matrix:

The combined mass matrix of the entire arm is obtained from the elemental mass matrices in datum coordinates.

The inertia forces acting on the j-th element of the arm are given by,

$$\{F_I\}_{(j)} = -[\bar{M}]_{(j)} \{\ddot{\bar{u}}\}_{(j)} \qquad (2.5.1)$$

Combining all such equations for different elements the following equation is obtained,

$$\{\bar{F}_I\} = -[\bar{\bar{M}}]\{\ddot{\bar{\bar{u}}}\} \qquad (2.5.2)$$

where,

$$\{\bar{F}_I\} = \{F_{I_1} \; F_{I_2} \ldots F_{I_j} \ldots . F_{I_{13}}\} \qquad (2.5.3)$$

$$[\bar{\bar{M}}] = \lceil \bar{M}_1 \; \bar{M}_2 \ldots \bar{M}_j \ldots \bar{M}_{13} \rfloor, \text{ and} \qquad (2.5.4)$$

$$\{\bar{\bar{u}}\} = \{\ddot{\bar{u}}_1 \; \ddot{\bar{u}}_2 \ldots . \ddot{\bar{u}}_j \ldots \ddot{\bar{u}}_{13}\} \qquad (2.5.5)$$

The elemental displacements $\{\bar{u}\}$ are expressed in terms of structural displacements $\{U\}$ by the relation[19]

$$\{\bar{u}\} = [A] \{U\} \qquad (2.5.6)$$

where $\{U\}$ is a vector of displacements on the assembled structure in the datum coordinates, and $[A]$ is a rectangular matrix in which every row consists of zeros except for a single term of unity, the position of which identifies that element of $\{\bar{u}\}$ which corresponds to the particular element of $\{U\}$. Making use of the Eqns. (2.5.2) to (2.5.5), it can be shown that the combined mass matrix for the complete structure regarded as a free body takes the form[19],

$$[M] = [A]^T [\bar{M}] [A] \qquad (2.5.7)$$

The transformation given in Eqn. (2.5.7) is computationally inconvenient to carry out. This operation is equivalent to the placing of elements from $[\bar{M}]_{(j)}$ in their correct positions in the larger framework of the matrix $[M]$ and then summing all the overlapping terms. This summation technique can be conveniently programmed for a computer. Hence, the transformation $[A]^T [\bar{M}] [A]$ is replaced by the foregoing summation procedure.

The skeleton structure of the combined mass matrix after the elimination of rows* and columns corresponding to rigid-body degrees-of-freedom, is given in Expression (2.5.9).

---

* Details given in Section (2.6).

ASSEMBLED MASS MATRIX, $\bar{M}$

	1–6	7–12	13–14	19–24	25–30	31–36	37–42	43–48	49–54	55–60	61–66	67–72	73–78
1–6	$m_{D1} + m_{A2}$	0	0	0	0	0	0	0	0	0	0	0	0
7–12		$m_{D2} + m_{A3}$	0	0	0	0	0	0	0	0	0	0	0
13–18			$m_{D4} + m_{A4}$	0	0	0	0	0	0	0	0	0	0
19–24				$m_{D4} + m_{A5}$	0	0	0	0	0	0	0	0	0
25–30					$m_{D5} + m_{A6}$	0	0	0	0	0	0	0	0
31–36						$m_{D6} + m_{A7}$	0	0	0	0	0	0	0
37–42							$m_{D7} + m_{A8}$	0	0	0	0	0	0
43–48								$m_{D8} + m_{A9}$	0	0	0	0	0
49–54									$m_{D9} + m_{A10}$	0	0	0	0
55–60		symmetric								$m_{D10} + m_{A11}$	0	0	0
61–66											$m_{D11} + m_{A12} + m_{A13}$	0	0
67–72												m_{D12}	0
73–78													m_{D13}

2.6 Assembled Stiffness Matrix

Stiffness matrices in datum coordinates for individual elements are combined to form the matrix relating the applied mechanical forces to the corresponding displacements on the assembled structure of the arm.

For an element j of the arm, the static forces are given by,

$$\{\overline{F}_s\} = [\overline{K}]_j \{\overline{u}\}_j \qquad (2.6.1.)$$

where all matrices refer to the datum coordinate system. Combining all such equations as (2.6.1) for different elements of the arm, the following matrix relationship is obtained,

$$\{\overline{F}_s\} = [\overline{K}]\{\overline{u}\} \qquad (2.6.2)$$

where,

$$\{\overline{F}_s\} = \{\overline{F}_{s_1}\ \overline{F}_{s_2} \ldots \overline{F}_{s_j} \ldots \overline{F}_{s_{13}}\} \qquad (2.6.3)$$

$$\{\overline{K}\} = [\overline{K}_1\ \overline{K}_2 \ldots \overline{K}_j \ldots \overline{K}_{13}] \qquad (2.6.4)$$

$$\{\overline{u}\} = \{\overline{u}_1\ \overline{u}_2 \ldots \overline{u}_j \ldots \overline{u}_{13}\} \qquad (2.6.5)$$

Making use of these equations, it can be shown that the stiffness matrix for the complete structure regarding the structure as a free body is obtained from the equation (2.6.7) (see Appendix III).

$$[K] = [A]^T [\overline{K}] [A] \qquad (2.6.7)$$

where $[A]$ is the same matrix as given in Eqn. (2.5.6).

The transformation given by Eqn. (2.6.7) is replaced by the summation procedure explained in the Section (2.5).

The external loading corresponding to the displacements $\{U\}$ is denoted by $\{P\}$ and is given by,

$$\{P\} = \{P_1 \; P_2 \; \ldots \; P_i \; \ldots \; P_{84}\} \qquad (2.6.8)$$

where P_i denotes an external force in the direction of the displacement U_i. The relation between $\{P\}$ and $\{U\}$ is given by (See Appendix III),

$$\{P\} = [A]^T [\bar{K}] [A] \{U\} = [K] \{U\} \qquad (2.6.9)$$

The load matrix $\{P\}$ constitutes a set of forces in static equilibrium and it includes the reaction forces. Considering overall equilibrium of the structure, there should be six dependent equations relating the forces $\{P\}$ corresponding to the rigid-body degrees-of-freedom since, all the forces in $\{P\}$ are not independent. This dependence renders the matrix $\{K\}$ singular[19] and hence the dependent equations are eliminated from the Eqn. (2.6.9). This is accompanied by assuming six zero displacements at some suitable points on the structure and then eliminating the corresponding rows and columns from the complete stiffness matrix $[K]$. The six displacements are chosen in such a way as to ensure that all the rigid-body degrees of freedom are completely restrained. For the radial drill-arm, the six displacements are selected at station point 1, where the arm is considered to be rigidly fixed. The first six rows and columns are then eliminated from the assembled stiffness matrix to obtain the reduced assembled stiffness matrix.

The skeleton structure for the complete stiffness matrix, with completely restrained rigid-body degrees-of-freedom, is shown in Expression (2.6.10).

2.7 Sectional Properties:

It is essential to know in detail the sectional properties of structural elements to find out their inertia and elastic properties.

The elemental sectional properties that are of interest are (i) area, (ii) position of centre of area, (iii) principal axes through the centre of area, and (iv) the second moments of area with respect to the principal axes.

A technique given in Ref. 12 is used to evaluate these. In this technique, the contour of each section is approximated by a sequence of straight lines and circular arcs which are convex or concave. The radius of the circular arcs is taken positive for convex curve and negative for concave curve.

The coordinates of all corners in the section are taken with respect to a suitable local coordinate system.

Let,

A denote area of cross section,

S_x and I_x denote first and second moments of the area respectively about x axis,

S_y and I_y denote first and second moments of the area respectively about y axis, and

I_{xy} denote the product moment of the area.

ASSEMBLED STIFFNESS MATRIX, $\overline{K}$

	1–6	7–12	13–18	19–24	25–30	31–36	37–42	43–48	49–54	55–60	61–66	67–72	73–78
1–6	$K_{D11} + K_{A2}$	K_{B2}	0	0	0	0	0	0	0	0	0	0	0
7–12		$K_{D2} + K_{A3}$	K_{B3}	0	0	0	0	0	0	0	0	0	0
13–18			$K_{D3} + K_{A4}$	K_{B4}	0	0	0	0	0	0	0	0	0
19–24				$K_{D4} + K_{A5}$	K_{B5}	0	0	0	0	0	0	0	0
25–30					$K_{D5} + K_{A6}$	K_{B6}	0	0	0	0	0	0	0
31–36						$K_{D6} + K_{A7}$	K_{B7}	0	0	0	0	0	0
37–42							$K_{D7} + K_{A8}$	K_{B8}	0	0	0	0	0
43–48								$K_{D8} + K_{A9}$	K_{B9}	0	0	0	0
49–54									$K_{D9} + K_{A10}$	K_{B10}	0	0	0
55–60			symmetric							$K_{D10} + K_{A11}$	K_{B11}	0	0
61–66											$K_{D11} + K_{A12} + K_{A13}$	K_{B12}	K_{B13}
67–72												K_{D12}	0
73–78													K_{D13}

These are calculated for the area enclosed between each contour line and respective coordinate axes. The sectional properties for the area enclosed between the upper and the lower contours are given by,

$$
\begin{aligned}
A &= \Sigma A_u - \Sigma A_l \\
S_x &= \Sigma S_{xu} - \Sigma S_{xl} \\
S_y &= \Sigma S_{yu} - \Sigma S_{yl} \\
I_x &= \Sigma I_{xu} - \Sigma I_{xl} \\
I_y &= \Sigma I_{yu} - \Sigma I_{yl} \\
I_{xy} &= \Sigma I_{xyu} - \Sigma I_{xyl}
\end{aligned}
\tag{2.7.1}
$$

where the suffixes u and l correspond to the upper and the lower contours respectively. (For detailed formulae, see Appendix I).

The various sections of the radial drill-arm have voids and to account for these voids, the foregoing technique is extended by treating the upper contour of the void as the lower contour of the section above the void and the lower contour of the void is taken as the upper contour of the section below.

The sectional centre of area (x_{ca}, y_{ca}) in the local coordinates is given by,

$$x_{ca} = S_y/A, \quad \text{and} \tag{2.7.2}$$

$$y_{ca} = S_x/A \tag{2.7.3}$$

The principal second moments of area are found out by transferring I_x, I_y and I_{xy} to a coordinate system (x_1, y_1) parallel to the local coordinate system having its origin at the centre of the area and then by rotating the (x_1, y_1) coordinate system through an angle θ given by,

$$\theta = 1/2 \tan^{-1} (2 I_{x1y1}/(I_{y1}-I_{x1})) \text{ radians} \quad (2.7.4)$$

θ is measured from the x_1 axis and it is taken positive in the counter clockwise direction. The principal second moments of area are evaluated from the expressions,

$$I_{x2} = I_{x1} \cos^2 \theta + I_{y1} \sin^2 \theta - I_{x1y1} \sin 2\theta \quad (2.7.5)$$

$$I_{y2} = I_{x1} \sin^2 \theta + I_{y1} \cos^2 \theta + I_{x1y1} \sin 2\theta \quad (2.7.6)$$

while $I_{x2y2} = 0$.

CHAPTER III

PREDICTION OF DYNAMIC RESPONSE OF THE ARM

3.1 General:

Machine tool structures are acted upon by static and dynamic loads in working conditions. Deflections caused by static loads are obtained from static flexibilities. For dynamic analysis, the response to harmonic excitations needs to be found out. Dynamic response is found out from mode shapes.

3.2 Natural Frequencies and Mode Shapes of the Arm:

The natural frequencies and the mode shapes of the arm are found out from the combined mass matrix and the assembled stiffness matrix.

The equation of free motion for an undamped structure is given by[13,15],

$$[M]\ \{\ddot{x}\} + [K]\ \{x\} = 0 \qquad (3.2.1)$$

where,

$[M]$ is the combined mass matrix,

$[K]$ is the assembled stiffness matrix, and

$\{x\}$ is the displacement vector.

For harmonic displacements, the displacement vector is given by,

$$\{x\} = \{X\} \sin w_n t \qquad (3.2.2)$$

Using Eqn. (3.2.2) in Eqn. (3.2.1), the equation of motion takes the form,

$$w_n^2 [M] \{X\} + [K] \{X\} = 0 \qquad (3.2.3)$$

where w_n^2 is square of natural frequency of the arm. Premultiplication of Eqn. (3.2.3) by $[M]^{-1}$ gives,

$$w_n^2 \{X\} + [M]^{-1} [K] \{X\} = 0 \qquad (3.2.4)$$

Here, $[M]^{-1} [K]$ is known as Dynamic Matrix. Eigenvalues of the dynamic matrix are squares of natural frequencies of the arm. Thematrix $[M]^{-1} [K]$ is not essentially symmetric and it is computationally inconvenient to evaluate eigenvalues of a non-symmetric matrix[17], especially when the matrix is of higher order. This necessitates the use of a more convenient method[18] wherein the dynamic matrix is essentially symmetric. Eigenvalues and eigenvectors of a symmetric matrix can be obtained by using Jacobi method (See Appendix IV).

Let,

$$[M] = [m] [m] \qquad (3.2.5)$$

where each element of $[m]$ is the square root of the corresponding element of $[M]$ ($[M]$ being a diagonal matrix). Substitution of Eqn. (3.2.5) into Eqn. (3.2.3) results in the following equation,

$$\omega_n^2 \; [M][M]\{X\} + [K]\{X\} = 0 \qquad (3.2.6)$$

Premultiplication of Eqn. (3.2.6) by $[M]^{-1}$ results in,

$$\omega_n^2 \; [M]\{X\} + [M]^{-1}[K][M]^{-1}[M]\{X\} = 0 \qquad (3.2.7)$$

Introducing a transformation,

$$\{Y\} = [M]\{X\} , \qquad (3.2.8)$$

Eqn. (3.2.7) takes the form,

$$\omega_n^2 \{Y\} + [M]^{-1}[K][M]^{-1}\{Y\} = 0 \qquad (3.2.9)$$

The matrix $[M]^{-1}[K][M]^{-1}$ is essentially symmetric and yields the same eigenvalues as $[M]^{-1}[K]$. On the other hand, the true eigenvectors (mode shapes) are obtained only after premultiplying $[M]^{-1}$ by the resulting eigenvectors.

3.3 Frequency Response:

The response of the arm to harmonic excitations is found out by summation of the responses of the individual modes, allowing for phase differences. The method involves a property of modes of vibration that under steady state conditions, the deflected shape of a structure excited by a set of oscillating forces may be expressed as the sum of factored mode shapes. These factors are determined from the mode shapes and the applied forces. However, the contribution of higher modes is negligible to the response of the structure and so, fourth and higher order modes are not considered to find out the response locus.

The response of the arm is represented in the form of harmonic response locus. Harmonic response locus is a plot of out-of-phase component against in-phase component of the displacement on the structure, frequency being marked along the length of the curve. The responses of individual modes depends on damping in the structure. In machine tools, for a given magnitude of damping, the difference between viscous and structural dampings is small and either kind could be used[3] for predicting responses without introducing any significant error in the computed loci. In the present analysis, viscous damping is chosen. Also, the separate analysis of each mode as a single degree-of-freedom system is mathematically exact in the case of undamped structures, but is not so in the presence of damping. However, in practice the assumption of an independent damping constant for each mode produces[3] good results.

It is known that undamped linear systems possess normal modes. It is not necessarily so in the case of damped systems. However, it is shown that if the damping matrix is linear combination of the stiffness and inertia matrices, the damped system will have normal modes[6,7]. A necessary and sufficient condition for a damped system to possess classical normal modes is that the damping matrix be diagonalised by the same transformation which uncouples the undamped system.

The equation of motion of a damped system may be written as,

$$[M]\{\ddot{x}\} + [C]\{\dot{x}\} + [K]\{x\} = \{f\} \sin wt \qquad (3.3.1)$$

where $\{f\}$ is the load vector.

Introducing a transformation,

$$[N]\{x\} = \{y\} \qquad (3.3.2)$$

where $[N] = [M]^{1/2}$ (3.3.3)

a diagonal matrix, substituting Eqn. (3.3.3) into Eqn. (3.3.1) and premultiplying by $[N]^{-1}$, Eqn. (3.3.1) takes the form,

$$[I]\{\ddot{y}\} + [N]^{-1}[C][N]^{-1}\{\dot{y}\} + [N]^{-1}[K]\{y\}$$
$$= [N]^{-1}\{f\} \sin wt \qquad (3.3.4)$$

Introducing the following notations,

$$[A] = [N]^{-1}[C][N]^{-1}, \qquad (3.3.5)$$

$$[B] = [N]^{-1}[K][N]^{-1}, \qquad (3.3.6)$$

and $\{F\} = [N]^{-1}\{f\}$ (3.3.7)

Eqn. (3.3.4) takes the form,

$$[I]\{\ddot{y}\} + [A]\{\dot{y}\} + [B]\{y\} = \{F\} \sin wt,$$

$[A]$, and $[B]$ being symmetric and positive definite.

Using another transformation,

$$\{y\} = [\phi]\{z\} \qquad (3.3.9)$$

it is possible to diagonalise $[A]$ and $[B]$ simultaneously both of them being symmetric and positive definite.

Substituting Eqn. (3.3.9) into Eqn. (3.3.8) and premultiplying by $[\phi]^T$, Eqn. (3.3.8) takes the form,

$$[\phi]^T[\phi]\{\ddot{a}\} + [\phi]^T[A][\phi]\{\dot{a}\} + [\phi]^T[B][\phi]\{a\}$$
$$= [\phi]^T\{F\} \quad \sin wt \qquad (3.3.10)$$

This transformation diagonalises[6] both A and B resulting in,

$$[\phi]^T[A][\phi] = [\diagdown 2\zeta_i w_{ni} \diagdown], \quad \text{and} \qquad (3.3.11)$$
$$[\phi]^T[B][\phi] = [\diagdown w_{ni}^2 \diagdown] \qquad (3.3.12)$$

where w_{ni} is the natural frequency of the i-th mode.

Substituting Eqn. (3.3.11) and Eqn. (3.3.12) into Eqn. (3.3.10), the latter takes the form,

$$[\phi]^T[\phi]\{\ddot{a}\} + [\diagdown 2\zeta_i w_{ni} \diagdown]\{\dot{a}\} + [\diagdown w_{ni}^2 \diagdown]\{a\} = \{F\} \sin wt \qquad (3.3.13)$$

where,

$$\{F\} = [\phi]^T\{F\} \qquad (3.3.14)$$

Equation (3.3.13) will be uncoupled only if,

$$[\phi]^T[\phi] = [I] \qquad (3.3.15)$$

i.e. $[\phi]$ is normalised matrix.

This means the transformation which simultaneously diagonalises both $[A]$ and $[B]$ is an orthogonal transformation.

Under these conditions, Eqn. (3.3.13) takes the form,

$$[I]\{\ddot{a}\} + [\diagdown 2\zeta_i w_{ni} \diagdown]\{\dot{a}\} + [\diagdown w_{ni}^2 \diagdown]\{a\} = \{F\} \sin wt \qquad (3.3.16)$$

The i-th of this system of uncoupled equations is,

$$\ddot{a}_i + 2\zeta_i w_{ni}\dot{a}_i + w_{ni}^2 a_i = F_i \sin wt \qquad (3.3.17)$$

The steady state response of the system in this mode is

given by,

$$q_i(t) = \frac{F_i \sin wt}{((w_{ni}^2 - w^2)^2 + 4\xi_i^2 w_{ni}^2 w^2)^{1/2}} \angle -\theta \qquad (3.3.18)$$

where θ is given by,

$$\tan \theta = \frac{2\xi_i w_{ni} w}{w_{ni}^2 - w^2} \qquad (3.3.19)$$

The response of the Radial Drill-Arm to a loading $\{f\}$ $\sin wt$ can be obtained by back transformation according to relations (3.3.9) and (3.3.2).

CHAPTER IV

RESULTS AND DISCUSSIONS

The theoretical aspects explained in the Chapters II and III are applied to two alternative designs of the arm of the radial drilling machine RD 6 to investigate into dynamic response of the arm. Brief indications about the computer programming developed for this purpose are given in Appendix V.

The following material properties for cast iron are used in the analysis[16].

Young's modulus (E) = 1.27×10^6 Kg/sq.cm.

Density (ρ) = 7.15 gm/cub.cm.

The rigidity modulus (G) of the material is calculated from the formula,

$$G = E/(2(1+\sigma))$$

where σ, the Poisson's ratio, is 0.27 for cast iron.

The static deflections of the arm to external loading of 2000 Kg thrust in vertical direction and 70 Kgm of twist in θ_1 direction at the drill point for the original and the alternative designs are shown in Fig. 9. These static deflections are nearly identical with slightly larger deflection for the alternative design.

The first ten natural frequencies for the original and the alternative designs are shown in Table 1. The type of displacement involved in each mode is also indicated in this Table.

The first four mode shapes for both the designs are shown in Figs. 10, 11, 12 and 13. In the first and the second modes (Figs. 10 and 11) the radial drill-arm is rocking in the Z and the Y (vertical) directions respectively. This is because the structure of the arm is weaker in the Z direction as compared to the Y direction. In the fourth mode (Figs. 12 and 13), the arm is twisting about its longitudinal axis. In the sixth mode, the natural frequencies and the mode shapes are identical for both the designs and this signifies that design changes of the arm do not influence chatter stability in the longitudinal (X) direction. The rest six modes are bending modes with one or more nodes.

Figs. 14, 15, 16 and 17 show the frequency response, at the station point 14 where the drill is mounted, in the vertical and the Z directions for both the original and the alternative designs. The responses (Figs. 14 and 15) in the vertical direction are nearly identical for both the designs. The responses (Figs.16 and 17) in the Z direction shows that the deflection corresponding to the first two natural frequencies are nearly identical where as the deflection corresponding to the third natural frequency is slightly larger for the alternative design.

The response loci at the drill point in the vertical and the Z directions for both the designs are shown in Figs. 18,19,20 and 21. In the vertical direction (Figs. 18 and 19) a large resonance is observed corresponding to the second natural frequency.

The amplitude corresponding to the second natural frequency is nearly three times to that corresponding to the first natural frequency in the Z directions (See Figs. 20 and 21).

Table 1

Natural Frequencies in CPS

Mode	Frequencies: Original Design	Frequencies: Alternative Design	Indication of Mode
1	1.88	1.87	Rocking, Z direction
2	3.39	3.38	Rocking, Y (Vertical) direction
3	9.35	9.19	Bending (one node) Z direction
4	12.05	12.02	Torsion, θ, direction
5	13.32	13.27	Bending (one node) Y direction
6	17.40	17.40	Rocking, X (longitudinal) direction.
7	20.78	20.65	Bending (2 nodes) Z direction
8	27.82	27.83	Bending (2 nodes) Y direction
9	28.33	28.69	Bending (3 nodes) Y direction
10	34.77	34.26	Bending (3 nodes) Z direction

Corresponding to the third natural frequency, in this direction, the amplitude is insignificant.

STATIC DEFLECTIONS

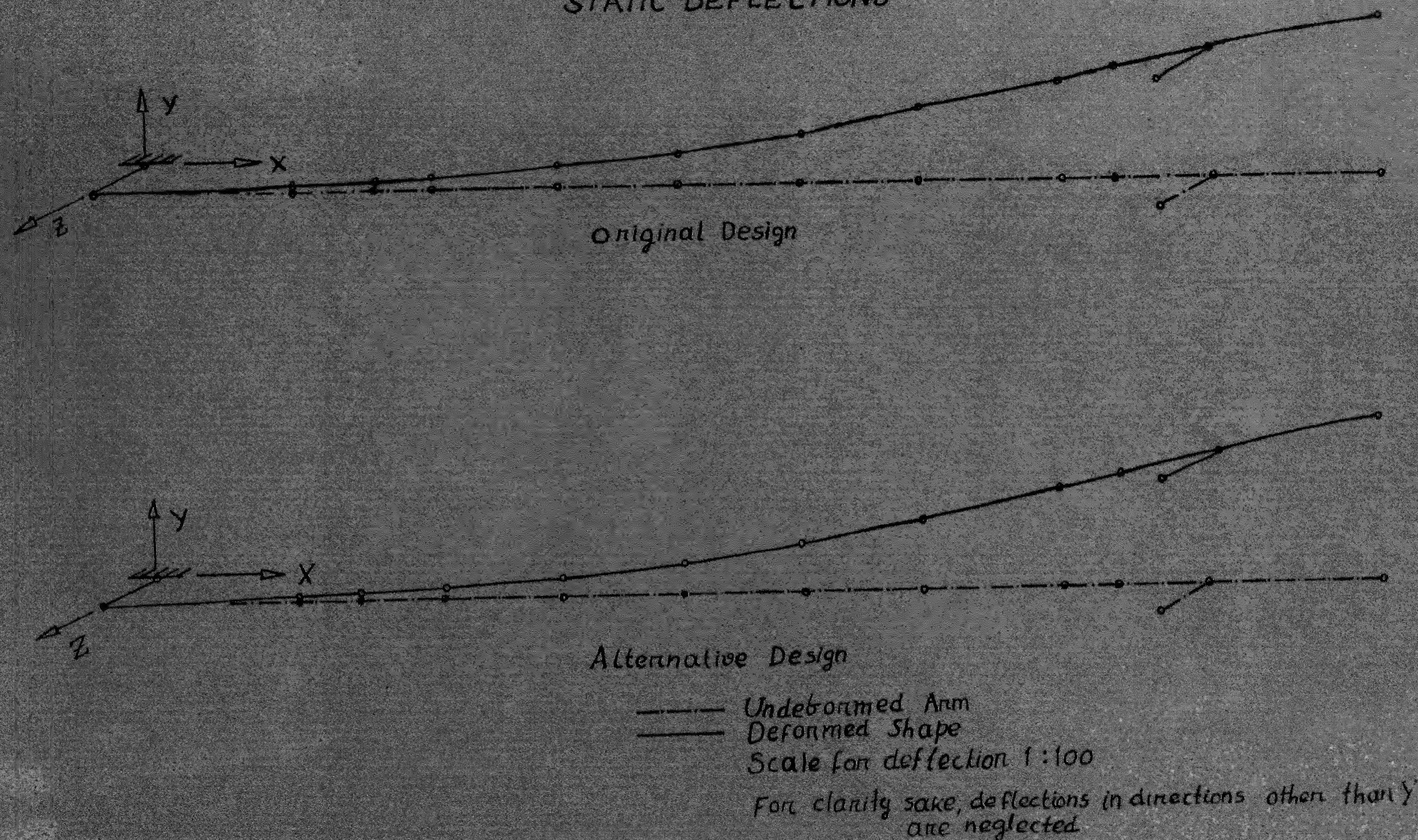

Fig. 9

ORIGINAL DESIGN

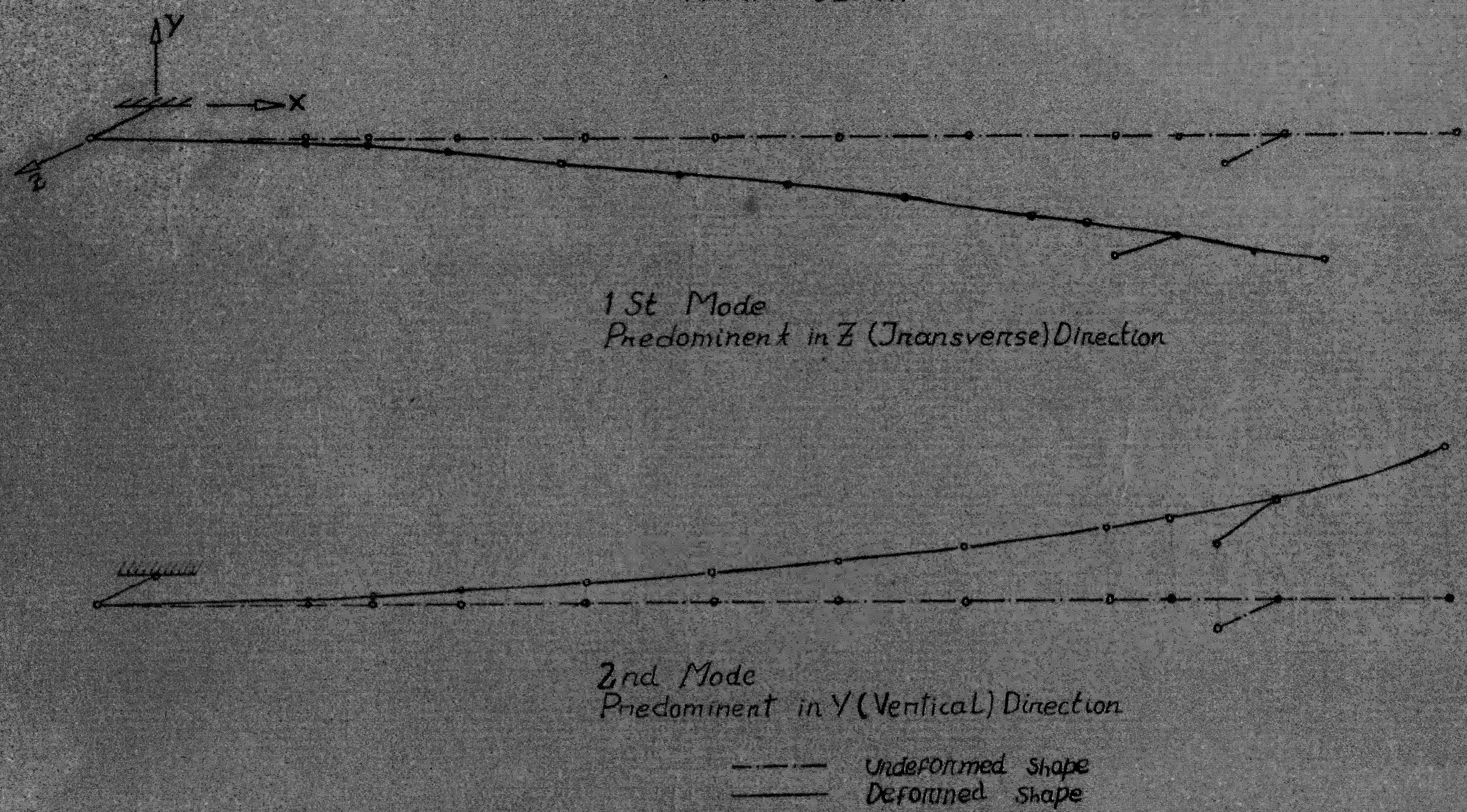

Fig 10

ALTERNATNE DESIGN

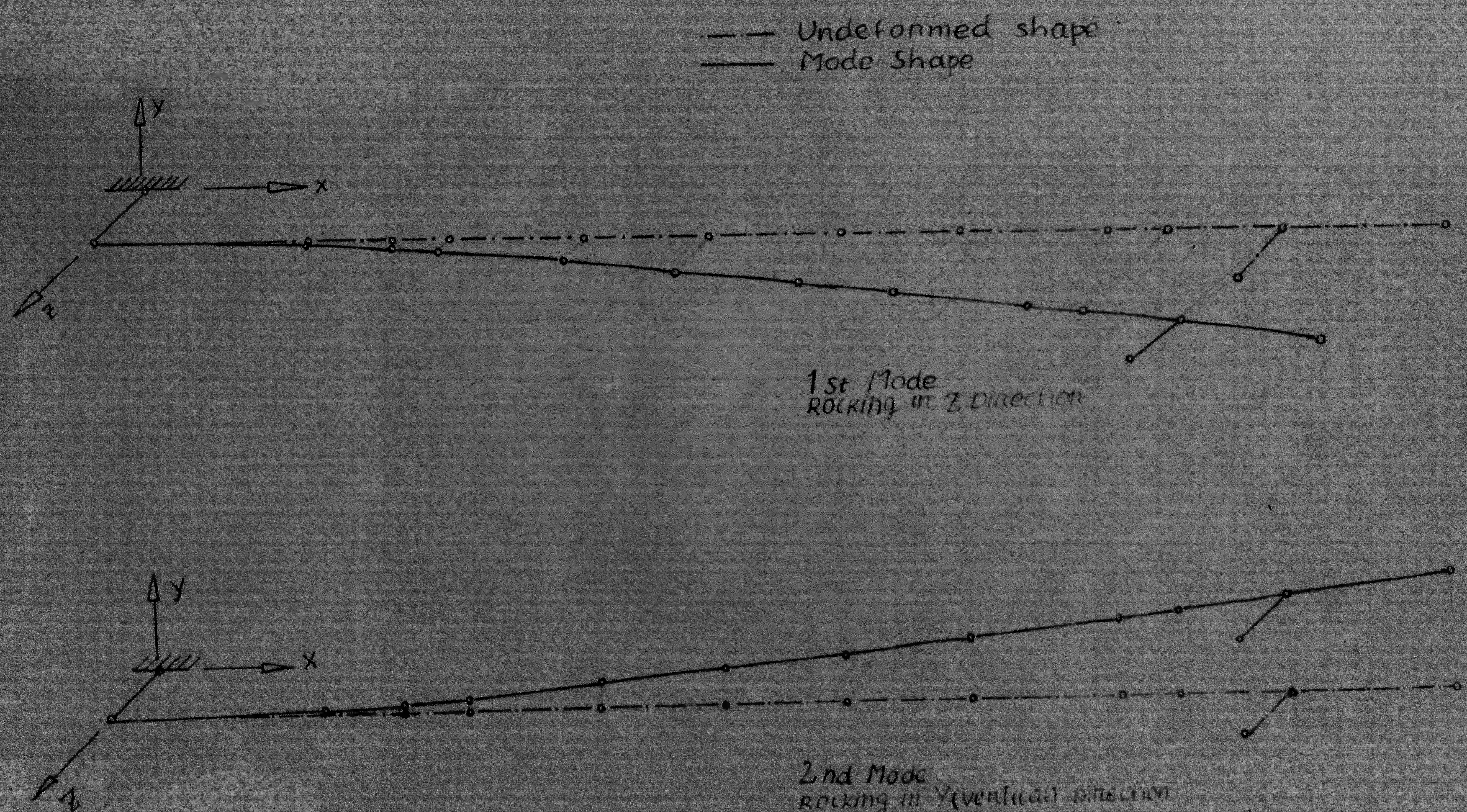

Fig 11

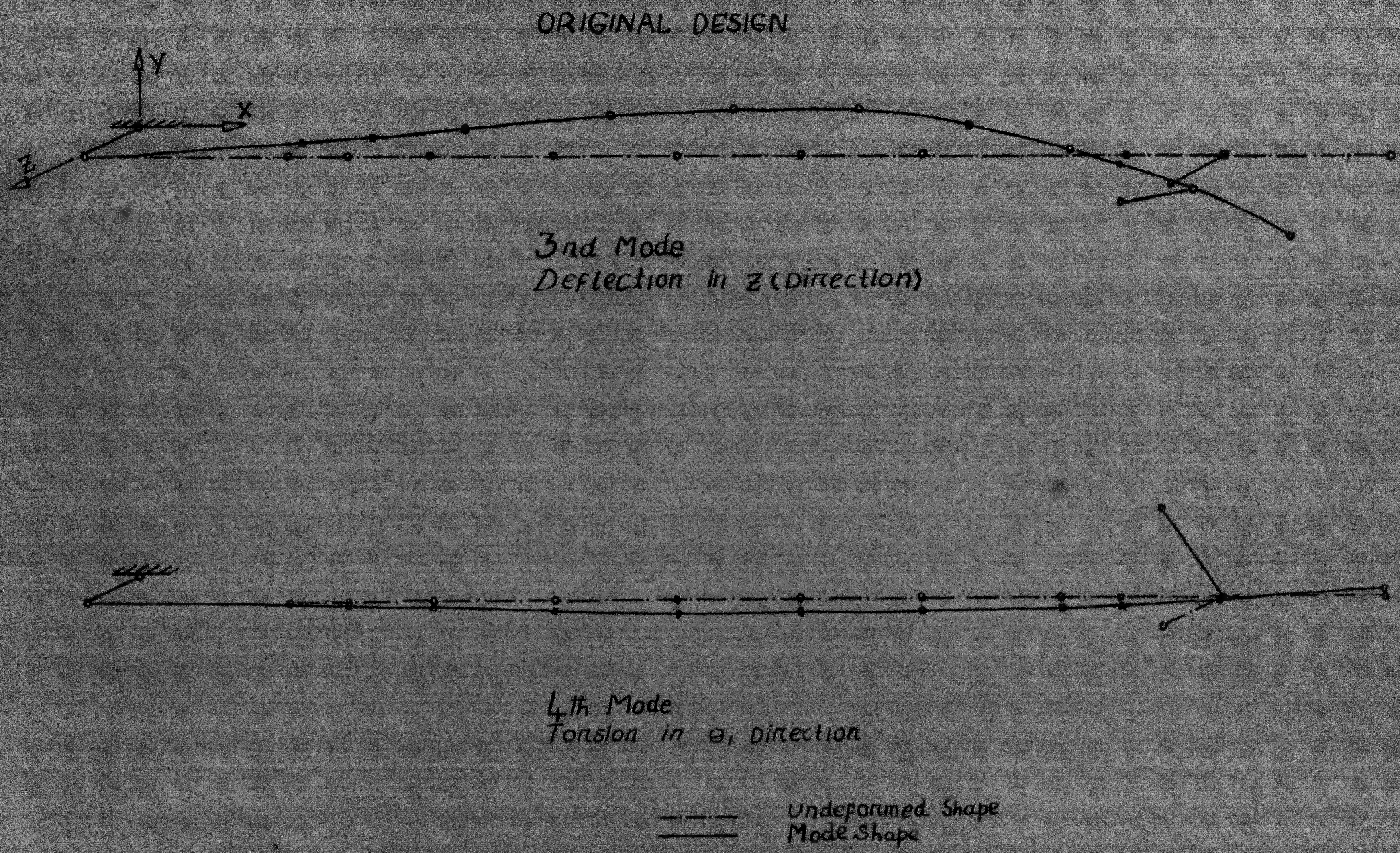
ORIGINAL DESIGN
Y
X
Z
3nd Mode
Deflection in Z (Direction)
4th Mode
Torsion in θ, Direction
Undeformed Shape
Mode Shape

Fig.12

ALTERNATIVE DESIGN

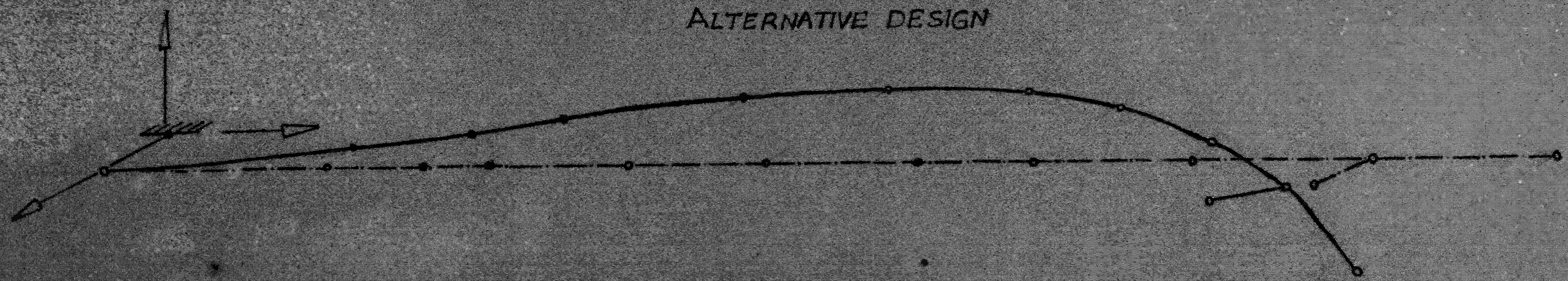

3 rd Mode
Deflection in Z Direction

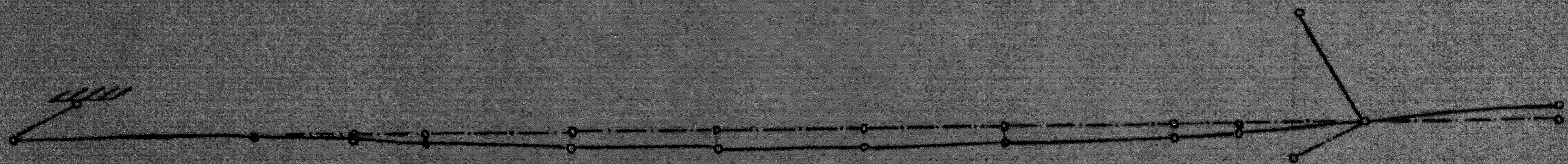

4 th Mode
Torsion in θ_1 Direction
— - — Undeflected Shape
——— Mode Shape

Fig. 13

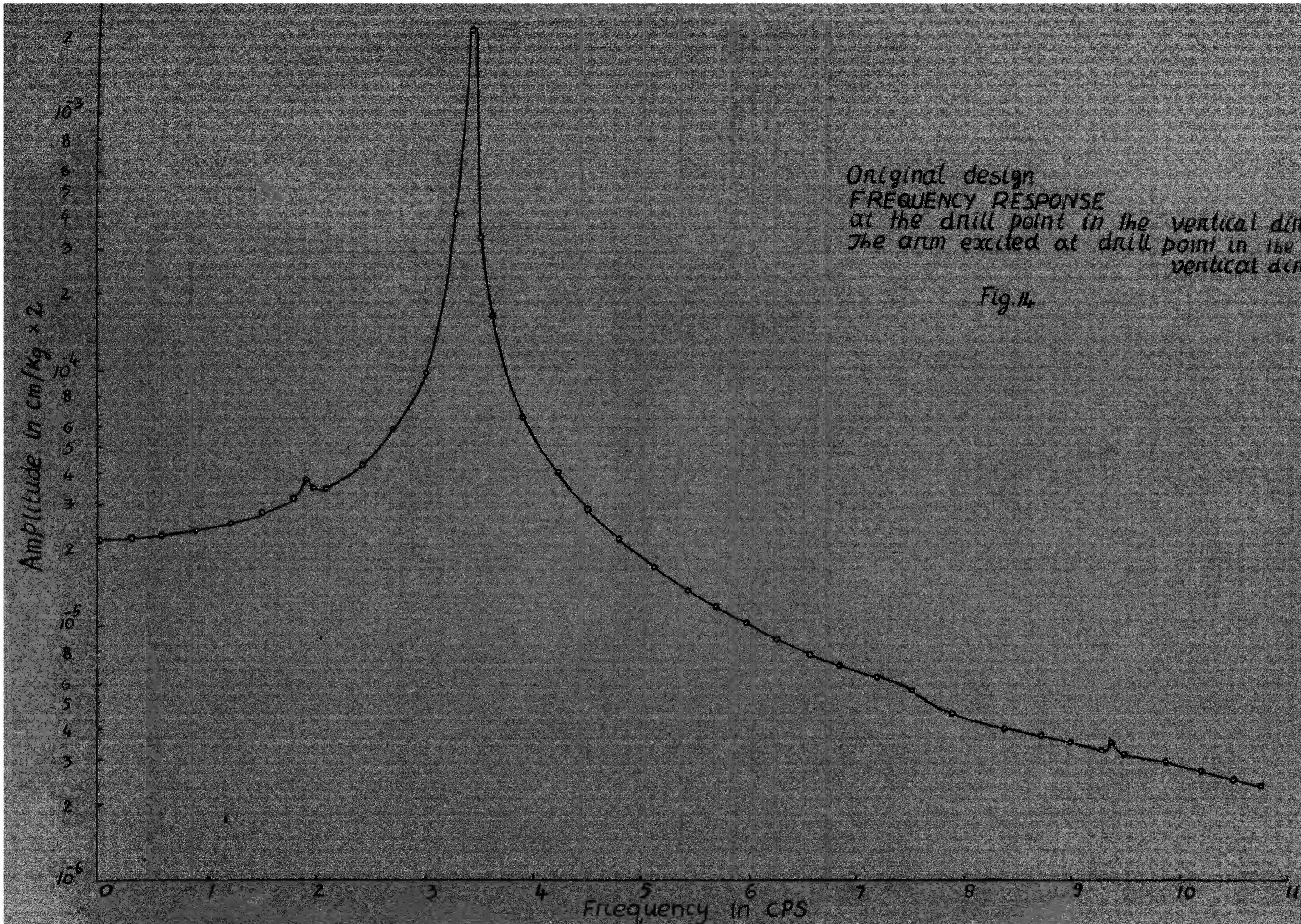

Original design
FREQUENCY RESPONSE
at the drill point in the vertical direction.
The arm excited at drill point in the vertical direction.

Fig.14

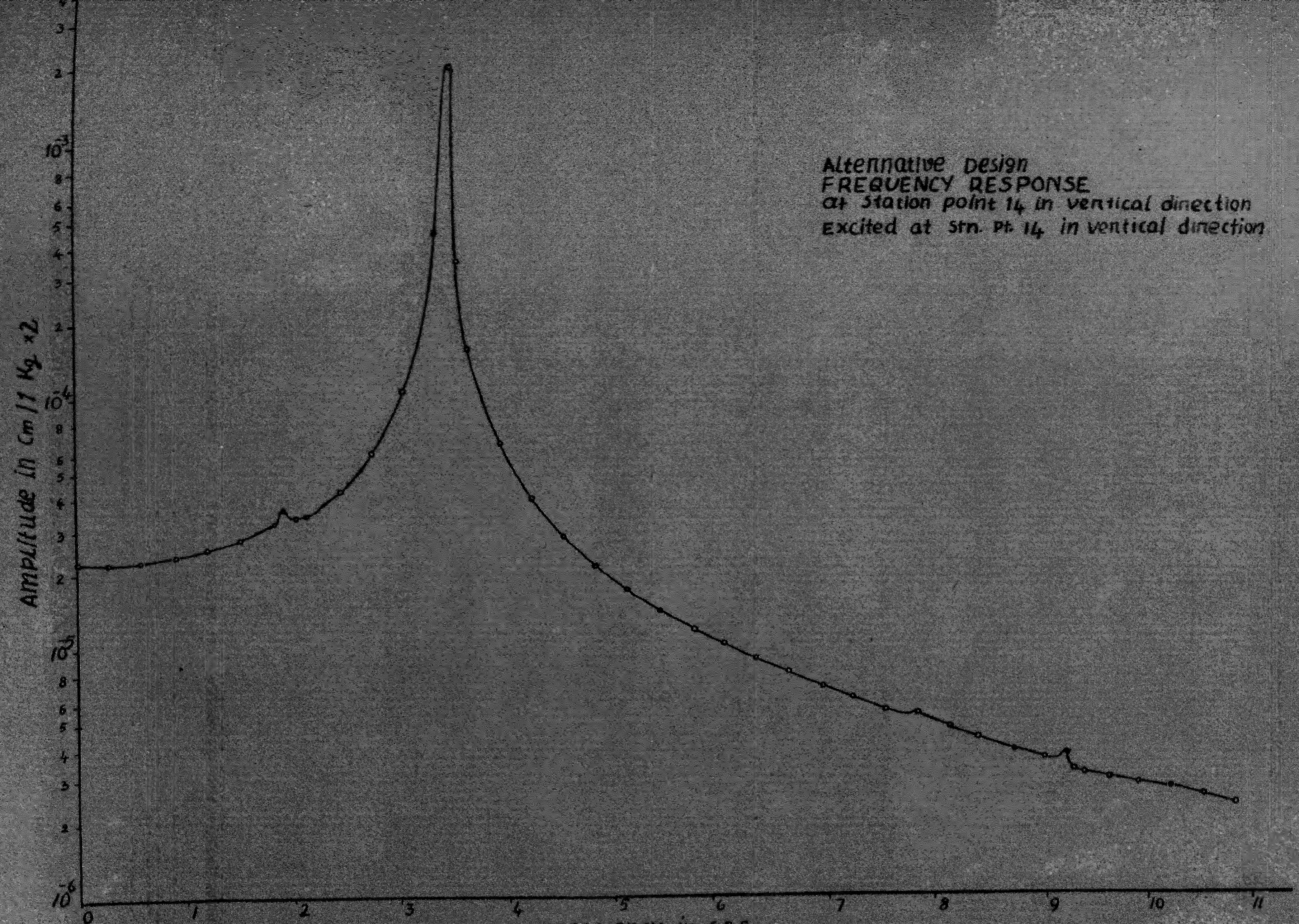
Alternative Design
FREQUENCY RESPONSE
at Station point 14 in vertical direction
Excited at Stn. Pt. 14 in vertical direction
Amplitude in Cm / 1 Kg. x2
Frequency in C.P.S.

Fig. 15

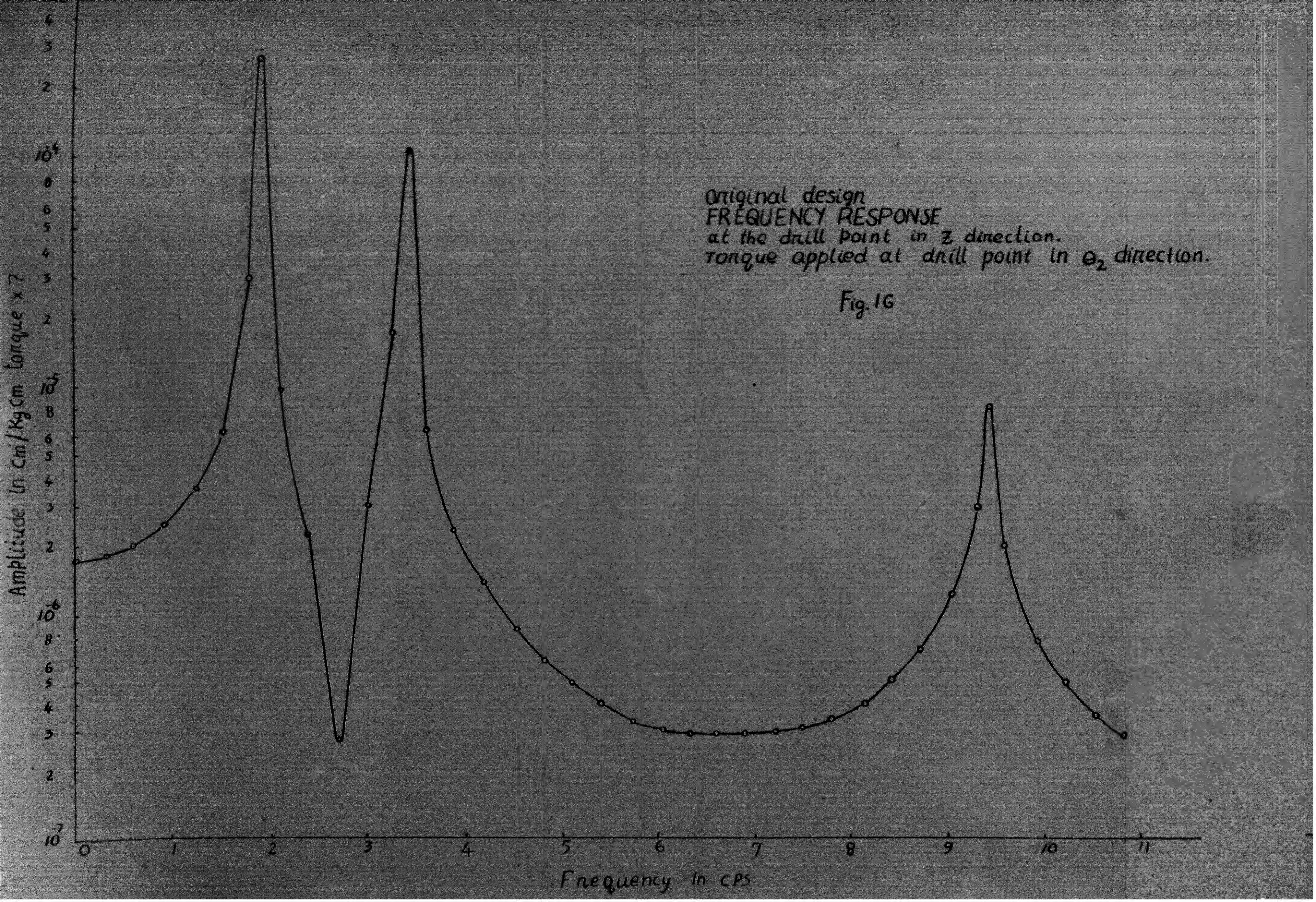
Original design
FREQUENCY RESPONSE
at the drill point in Z direction.
Torque applied at drill point in θ_2 direction.
Amplitude in cm/Kg cm torque x 7
Frequency in CPS
0
1
2
3
4
5
6
7
8
9
10
11
Fig. 16

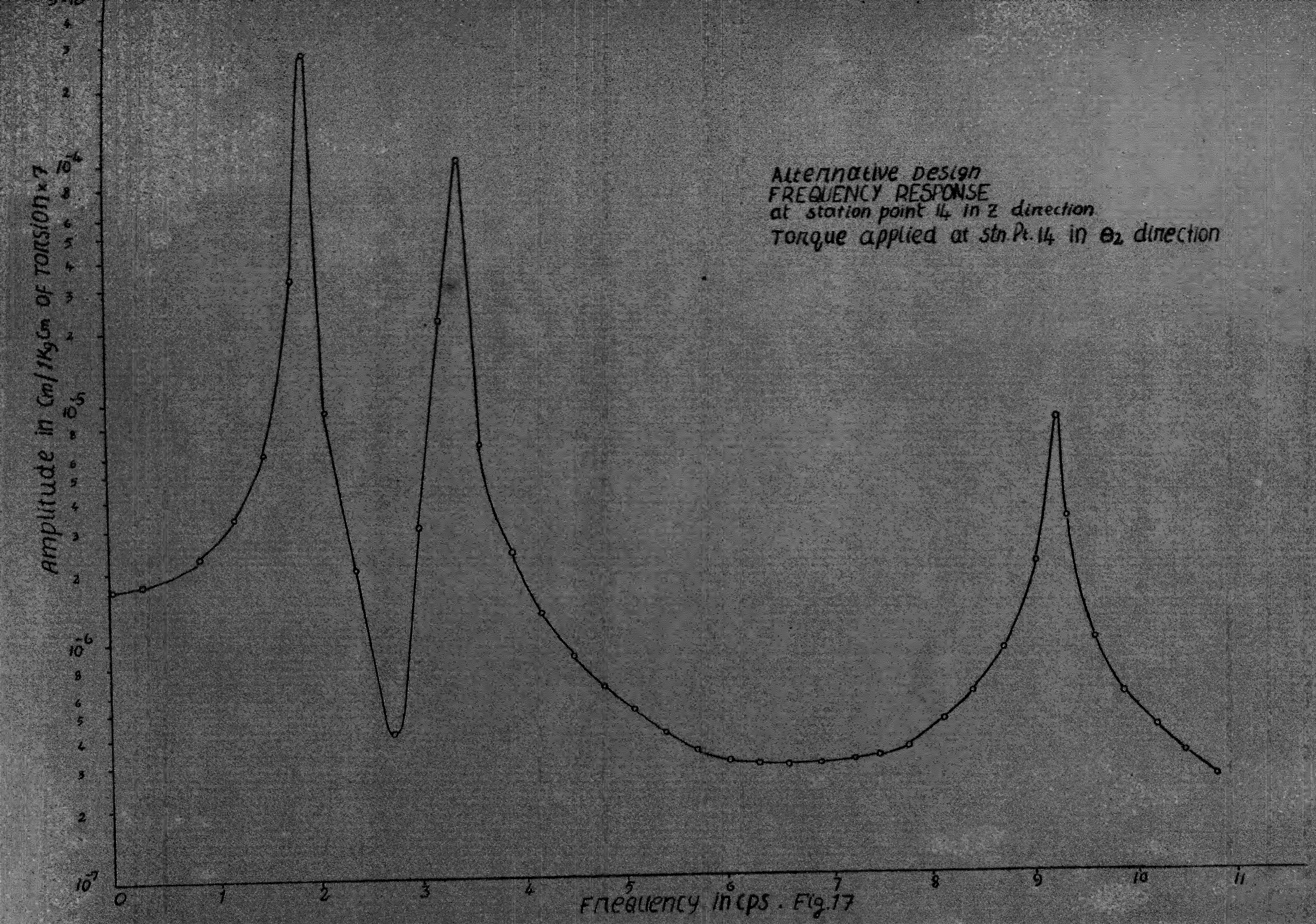
Alternative Design
FREQUENCY RESPONSE
at station point 14 in z direction
Torque applied at Stn.Pt. 14 in θ2 direction
Amplitude in Cm/1Kg Cm of Torsion×7
Frequency in cps . Fig.17

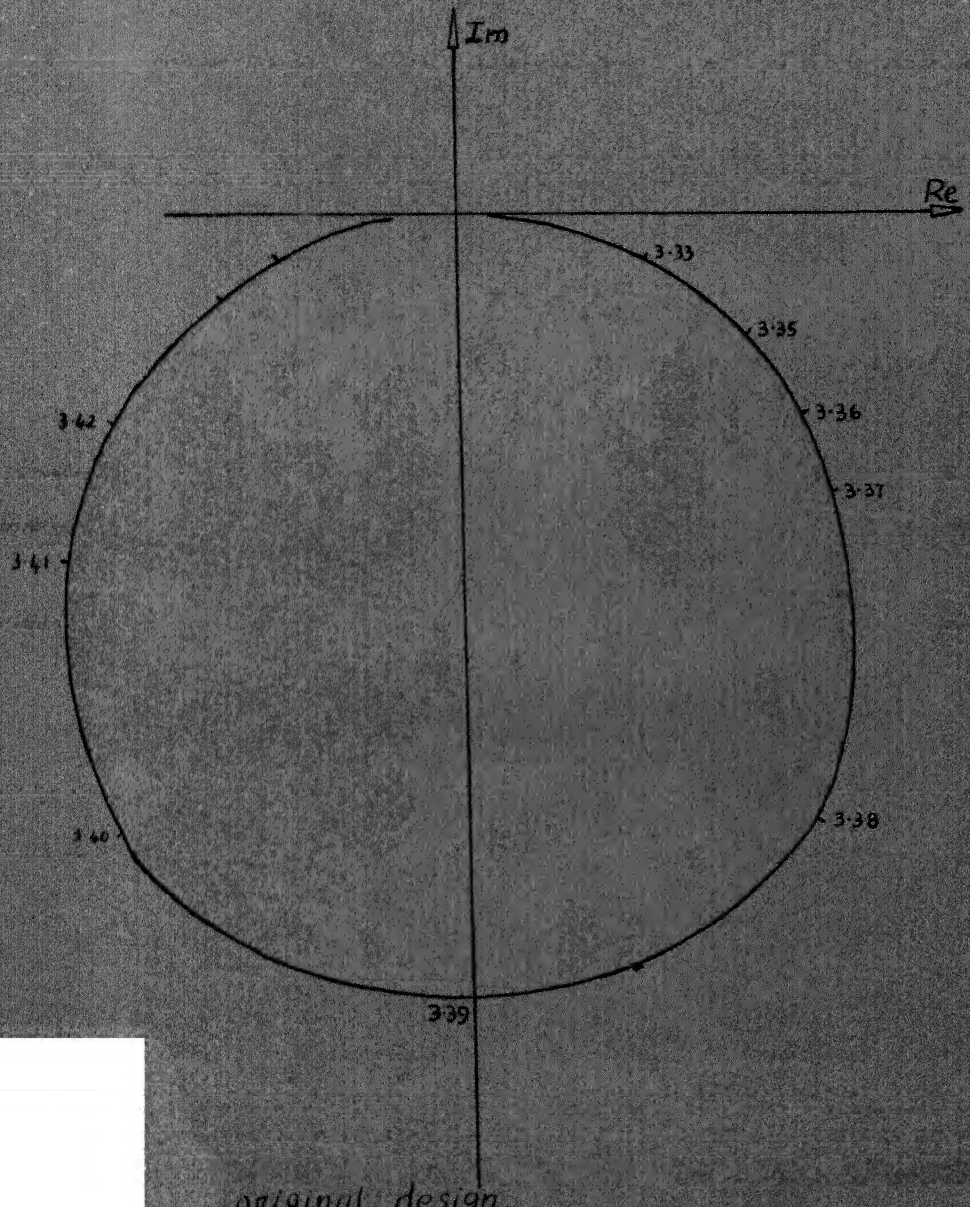

original design.
HARMONIC RESPONSE LOCUS
for the arm at the drill point in vertical direction.
Frequency in CPS . scale $1 \cdot 10^{-4}$

Fig 18

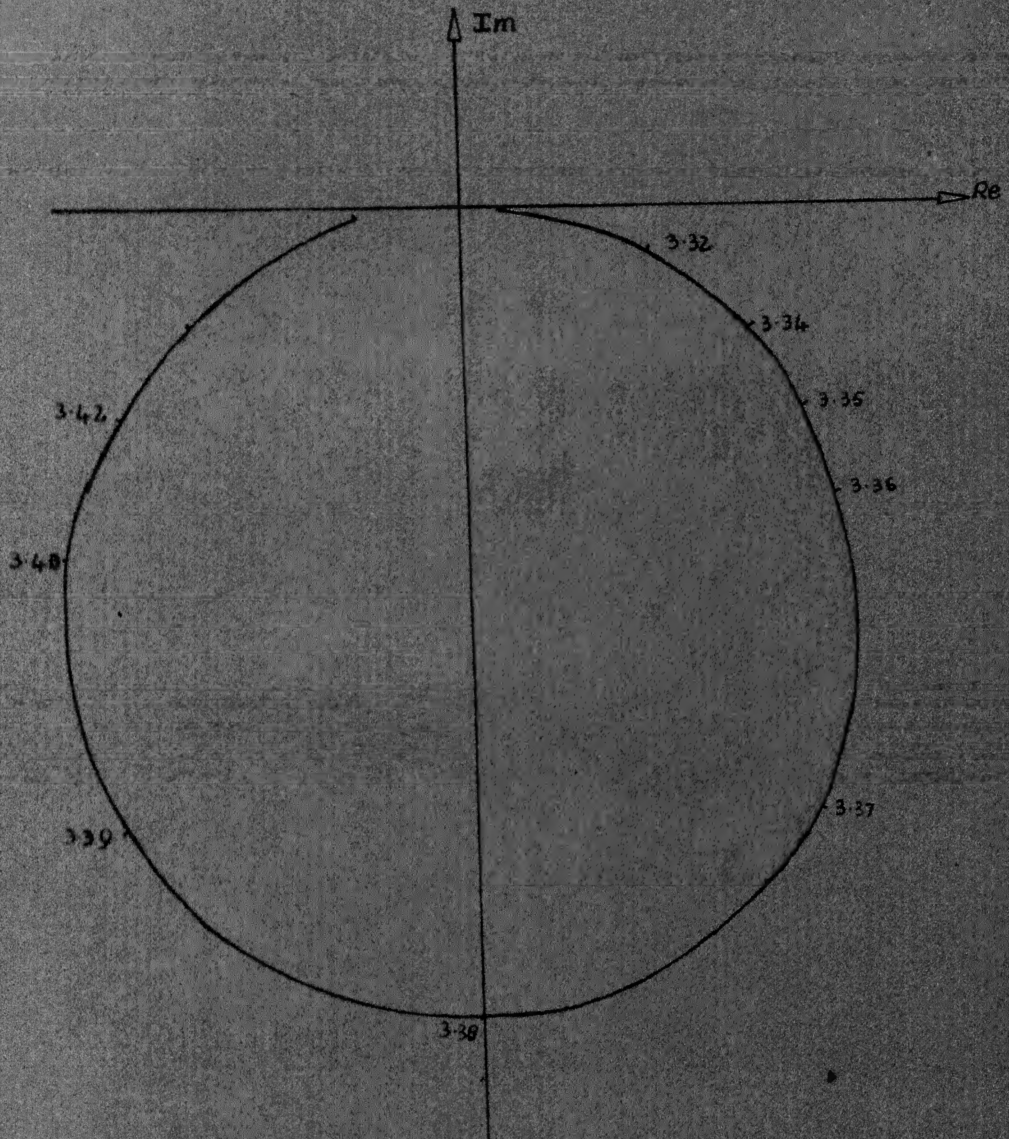

Alternative design
HARMONIC RESPONSE LOCUS
For the arm at drill point in vertical direction
Frequency in CPS. scale 1: 1×10^{4}

Fig. 19

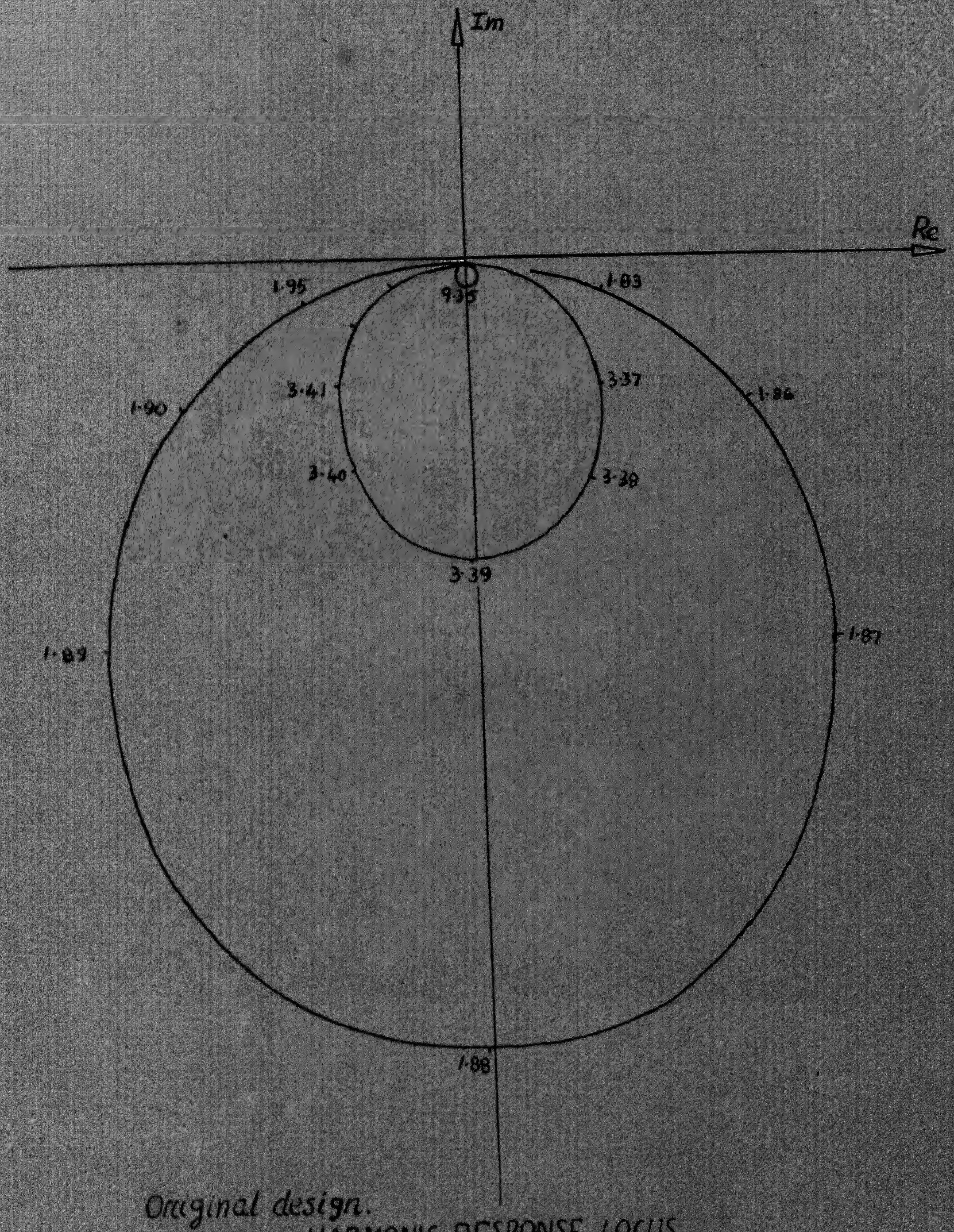

Original design.
HARMONIC RESPONSE LOCUS
For the arm at drill point in Z direction.
Frequency in CPS. Scale 1:3·6x10⁻⁶
Fig. 20

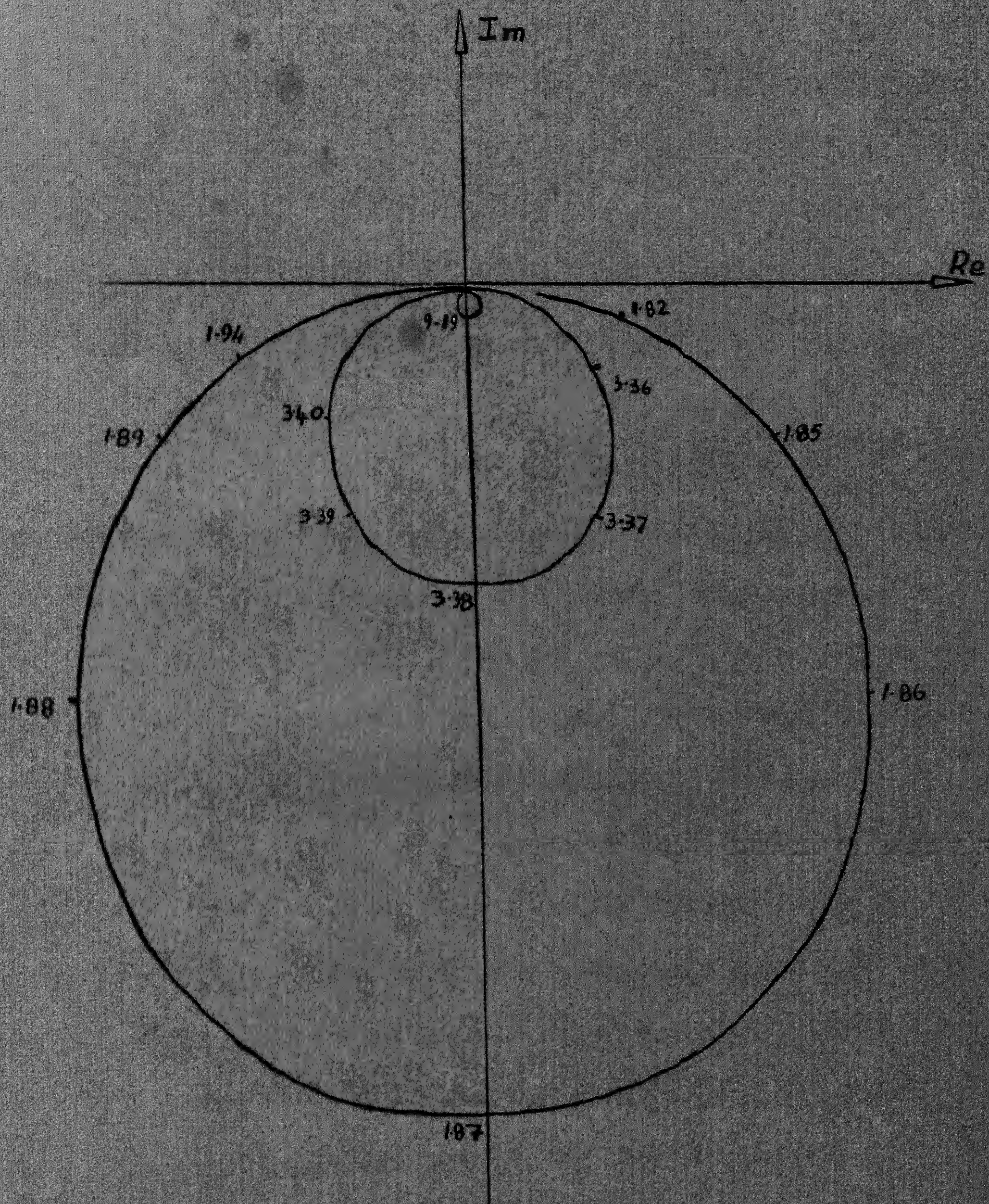

Alternative design.
HARMONIC RESPONSE LOCUS
for the arm at drill point in 2 direction.
Frequency in CPS. scale $1:3{\cdot}6\times10^{-6}$

Fig 21

CHAPTER VI

CONCLUSIONS AND SUGGESTIONS FOR FUTURE WORK

It is concluded that the arm of the radial drilling machine RD 6 has nearly identical static and dynamic responses for the original and the alternative designs.

Lumped-mass model has been used in this work to investigate into the dynamic response of the arm. Actually, a more realistic representation of the original continuous structure can be obtained by using a distributed-mass model rather than by a lumped-mass model. The radial drill-arm has box structure with complicated ribbing. So, finite element analysis of the arm is better than lumped-mass analysis for more accurate prediction of the dynamic response of the arm. The actual structural details of the arm near its fixed end have been slightly altered in the present work for computational convenience only. These actual structural details can be taken into consideration. The first approximate values of the shear deformation parameters have been found in the present work. The effect of shear deformation on the response of the arm can be fully taken into consideration by accurately estimating the values of the shear deformation parameters. Lastly, investigations can be carried out with a better estimation of the nature and the magnitude of damping present in the arm.

REFERENCES

1. S. Taylor and S.A. Tobias, Lumped-Constant Method for the Prediction of Vibration Characteristics of Machine Tool Structures, Advances in Machine Tool Design and Research, September, 1964, pp. 37.

2. S. Taylor, A Computer Analysis of Open Side Planning Machine, Advances in Machine Tool Design and Research, Sept. 1965, pp. 197.

3. S. Taylor, The Design of Machine Tool Structures Using a Digital Computer, Advances in Machine Tool Design and Research, September, 1966, pp. 369.

4. S. Taylor and S.A. Tobias, Computer Methods for the Structural Analysis of Machine Tools, Annals of C.I.R.P., Pergamon Press, 1969.

5. F.A. Leckie and G.M. Lindberg, The Effect of Lumped Parameters on Beam Frequencies, Aeronautical Quarterly, Vol. 14, 1963, pp. 224.

6. T.K. Caughey, Classical Normal Modes in Damped Linear Dynamic Systems, Journal of Applied Mechanics, Vol. 27, 1960, pp. 269.

7. T.K. Caughey, and M.E.J. O'Kelly, Classical Normal Modes in Damped Linear Systems, Journal of Applied Mechanics, Vol. 32, 1965, pp. 583.

8. A. Cowley and M.A. Fawcett, The Analysis of a Machine Tool Structure by Computing techniques, Advances in Machine Tool Design and Research, Pergamon Press, 1967.

9. J.P. Gurney and S.A. Tobias, A Graphical Analysis of Regenerative Machine Tool Instability, Vol. 84, Trans. ASME, Journal of Engg. for Industry, Feb, 1962, pp. 103.

10. H.E. Merritt, Theory of Self-Excited Machine Tool Chatter, Journal of Engineering for Industry, Trans. ASME, Vol. 87, 1965, pp. 447.

11. C. Andrews and S.A. Tobias, A Critical Comparison of Two Current Theories of Machine Tool Chatter, Int. Journal of Machine Tool Design and Research, Vol. 1, 1961, pp. 325.

12. J.C. Maltbaek, Moments of Area of Aerofoil Sections, Aircraft Engineering Vol. 33, December, 1961, pp. 351.

13. S. Timoshenko, Vibration Problems in Engineering, Van Nostrand Company, Inc. 1967.

14. S.A. Tobias, Machine Tool Vibrations, Blackie, 1965.

15. W.C. Hurty and M.F. Rubinstein, Dynamics of Structures, Prentice Hall of India, 1967.

16. A.P. Thurston, Molesworth's Handbook of Engineering Formulae and Data, E. and F.N. Spon Ltd., 1951.

17. Wilkinson, Algebraic Eigenvalue Problem, Clarendon Press-Oxford, 1965.

18. Shan S. Kuo, Numerical Methods and Computers, Addison-Wesley, 1965.

19. J.S. Przemieniecki, Theory of Matrix Structural Analysis, McGraw-Hill Book Co. (N.Y.), 1968.

APPENDIX I

FORMULAE FOR MOMENTS OF AREA BELOW A STRAIGHT LINE

Let (x_1, y_1) and (x_2, y_2) be the coordinates of the successive points on the contour of a section. The sectional properties of the area enclosed between the straight line joining these two points and the x axis are obtained from the following formulae.

Letting,

$$a = x_2 - x_1 , \quad \text{and} \qquad \text{(A 1.1)}$$

$$b = y_2 - y_1 \qquad \text{(A 1.2)}$$

area A, first moments of area M_x and M_y about x and y axes respectively, second moments of area I_x and I_y about x and y axes respectively, and product moment of area I_{xy} are given by,

$$A = \int_{x_1}^{x_2} y \, dx = a(y_1 + b/2) \qquad \text{(A 1.3)}$$

$$M_x = 1/2 \int_{x_1}^{x_2} y^2 \, dx = a\,(y_1(y_1 + b) + b^2/3)/2 \qquad \text{(A 1.4)}$$

$$M_y = \int_{x_1}^{x_2} yx \, dx = a(x_1(y_1+b/2) + a(y_1+2b/3)/2) \qquad \text{(A 1.5)}$$

$$I_x = 1/3 \int_{x_1}^{x_2} y^3 \, dx = a(y_1^2\,(y_1 + 3b/2) + b^2(y_1+b/4))/3 \qquad \text{(A 1.6)}$$

$$I_y = \int_{x_1}^{x_2} yx^2 \, dx = a(x_1^2(y_1+b/2) + ay_1(x_1+a/3) + 2ab\,(x_1 + 3a/8)/3) \qquad (A\ 1.7)$$

$$I_{xy} = 1/2 \int_{x_1}^{x_2} xy^2 \, dx = a(y_1^2(x_1+a/2) + bx_1(y_1+b/3) + 2ab\,(y_1+3b/8)/3)/2 \qquad (A\ 1.8)$$

APPENDIX II

INERTIA PROPERTIES OF ARM - ELEMENTS

$$m_1 = 1/2 \quad AL/2 \qquad \text{(A 2.1)}$$

Let I_{mxx}, I_{myy} and I_{mzz} denote mass moments of inertia about x, y and z axes respectively.

$$I_{mxx} = /g \int_v (z^2 + y^2)\, dv$$

where v is volume of half the element.

$$I_{mxx} = /g\,(z^2\, dx\, dy\, dz + y^2\, dx\, dy\, dz)$$

$$= /g\,(I_y\, L/2 + I_z\, L/2) \qquad \text{(A 2.2)}$$

$$I_{myy} = /g \int_v (x^2 + z^2)\, dv$$

$$= /g \int_v (x^2 + z^2)\, dx\, dy\, dz$$

$$= /g\, \int(AL^3/24 + I_y\, L/2) \qquad \text{(A 2.3)}$$

$$I_{mzz} = /g \int_v (y^2 + x^2)\, dx\, dy\, dz$$

$$= /g\, (AL^3/24 + I_z\, L/2) \qquad \text{(A 2.4)}$$

APPENDIX III

RELATION BETWEEN ASSEMBLED STIFFNESS MATRIX AND ELEMENTAL STIFFNESS MATRICES

The matrix equation relating element forces to element displacements is given by,

$$\{F_e\} = [K]\{\bar{u}\} \qquad (A\ 3.1)$$

The vector corresponding to external loading is,

$$\{P\} = \{P_1\ P_2 \ldots P_j \ldots P_m\} \qquad (A\ 3.2)$$

where m is the total number of degrees of freedom of the structure. The matrix relating element displacements to assembled structure displacements is,

$$\{\bar{u}\} = [A]\{U\} \qquad (A\ 3.3)$$

Introducing virtual displacements we get,

$$\{\delta\bar{u}\} = [A]\{\delta U\} \qquad (A\ 3.4)$$

Virtual work, for the virtual displacements $\{\delta U\}$, is given by,

$$\delta W = \{\delta U\}^T\{P\} \qquad (A\ 3.5)$$

The virtual strain energy is given by,

$$\delta U_i = \sum_j \{\delta\bar{u}_{(j)}\}^T\{F_e\}_{(j)} = \{\delta\bar{u}\}^T\{F_e\} \qquad (A\ 3.6)$$

From the principle of virtual work,

$$\delta W = \delta U_i$$

Hence,

$$\{\delta U\}\{P\} = \{\delta \bar{U}\}^T \{\bar{F}_s\} \qquad (A\ 3.7)$$

Substituting Eqn. (A 3.4) in (A 3.7) the following relation is obtained,

$$\{\delta U\}^T \left(\{P\} - [A]^T \{\bar{F}_s\}\right) = 0 \qquad (A\ 3.8)$$

hence,

$$\{P\} = [A]^T \{\bar{F}_s\} \qquad (A\ 3.9)$$

Substituting Eqns. (A 3.1) and (A 3.3) in (A 3.9) the following relation is obtained,

$$\{P\} = [A]^T [\bar{K}] \{\bar{u}\}$$

$$= [A]^T [\bar{K}] [A] \{U\} \qquad (A\ 3.10)$$

Denoting $[A]^T [\bar{K}] [A]$ by $[K]$, Eqn. (A 3.10) takes the form,

$$\{P\} = [K] \{U\} \qquad (A\ 3.11)$$

APPENDIX IV

JACOBI METHOD FOR FINDING EIGENVALUES AND EIGENVECTORS OF A SYMMETRIC MATRIX

It is convenient to use Jacobi method to determine eigenvalues and eigenvectors of a hermitian matrix. Jacobi method is essentially an iterative method. This method is based on the principle that a hermitian matrix $[A_0]$ always has linear elementary devisors and there is always a unitary matrix $[R]$ such that,

$$[R]\ [A]\ [R]^{*} = \text{diag}\ (\lambda_i) \qquad (A\ 4.1)$$

For a real symmetric matrix, the matrix $[R]$ is real and is, therefore, an orthogonal matrix.

In the Jacobi method, the original matrix is transformed to diagonal form by a sequence of plane rotations. For a real symmetric matrix, real plane rotations are used. The rotation is carried out in a plane (p, q) which corresponds to the off-diagonal element of maximum modulus. After k number of rotations, the original matrix takes the form,

$$[A_k] = [R_k]\ [A_{k-1}]\ [R_k]^{T} \qquad (A\ 4.2)$$

The angle θ of rotation is chosen so as to reduce the (p, q) element of $[A_{k-1}]$ to zero. An element reduced to zero in a particular rotation is generally made non-zero in a subsequent

rotation. This makes the process iterative. The process is truncated when the largest off-diagonal element is negligible in modulus for working accuracy.

For p less than q, the matrix R_k is given by,

$$
\begin{aligned}
R_{pp} &= R_{qq} = \cos\theta \\
R_{pq} &= -R_{qp} = \sin\theta \\
R_{ii} &= 1 \quad (i \neq p, q) \\
R_{ij} &= 0 \quad \text{otherwise}
\end{aligned}
\qquad \text{(A 4.3)}
$$

$[A_k]$ in Eq. (A 4.2) is symmetric and $[A_k]$ and $[A_{k-1}]$ differ only in rows and columns of p and q. The modified elements are given by,

$$a_{ip}^{(k)} = a_{pi}^{(k)} = a_{ip}^{(k-1)} \cos\theta + a_{iq}^{(k-1)} \sin\theta \quad i \neq p, q \qquad \text{(A 4.4)}$$

$$a_{iq}^{(k)} = a_{qi}^{(k)} = -a_{ip}^{(k-1)} \sin\theta + a_{iq}^{(k-1)} \cos\theta \quad i \neq p, q \qquad \text{(A 4.5)}$$

$$a_{pp}^{(k)} = a_{pp}^{(k-1)} \cos^2\theta + 2a_{pq}^{(k-1)} \cos\theta \sin\theta + a_{qq}^{(k-1)} \sin^2\theta \qquad \text{(A 4.6)}$$

$$a_{qq}^{(k)} = a_{pp}^{(k-1)} \sin^2\theta - 2a_{pq}^{(k-1)} \cos\theta \sin\theta + a_{qq}^{(k-1)} \cos^2\theta \qquad \text{(A 4.7)}$$

$$a_{pq}^{(k)} = a_{qp}^{(k)} = (a_{qq}^{(k-1)} - a_{pp}^{(k-1)}) \cos\theta \sin\theta + a_{pq}^{(k-1)} (\cos^2\theta - \sin^2\theta) \qquad \text{(A 4.8)}$$

Expression for θ is obtained by putting $a_{pq}^{(k)} = a_{qp}^{(k)} = 0$ in (A 4.8). θ is given by,

$$\tan 2\theta = 2a_{pq}^{(k-1)}/(a_{pp}^{(k-1)} - a_{qq}^{(k-1)}) \qquad (A\ 4.9)$$

It can be written that,

$$[A_k] = \text{diag:}\ (a_{ii}^{(k)}) + [E_k] \qquad (A\ 4.10)$$

where $[E_k]$ is a symmetric matrix of off-diagonal elements. It can be shown that,

$$||E_k||_E \rightarrow 0 \qquad (A\ 4.11)$$

and $\quad [A_k] \rightarrow \text{diag:}\ (\lambda_i) \qquad (A\ 4.12)$

as $k \rightarrow \infty$.

In Eqn. (A 4.12) diag: (λ_i) is a fixed diagonal matrix, λ_i being eigenvalues of the original matrix, and hence of all $[A_k]$.

If the final rotation is represented by $[R_f]$, then,

$$(R_f \ldots R_2 R_1)(A_0)(R_1^T\ R_2^T \ldots R_f^T) = \text{diag:}\ (\lambda_i) \qquad (A\ 4.13)$$

Therefore, the eigenvectors of the original matrix $[A_0]$ are the column vectors of a matrix $[P_f]$ defined by,

$$[P_f] = [R_1^T\ R_2^T \ldots R_f^T] \qquad (A\ 4.14)$$

APPENDIX V

COMPUTER PROGRAM FOR THE THEORETICAL ASPECTS OF THE WORK

Flow diagram,

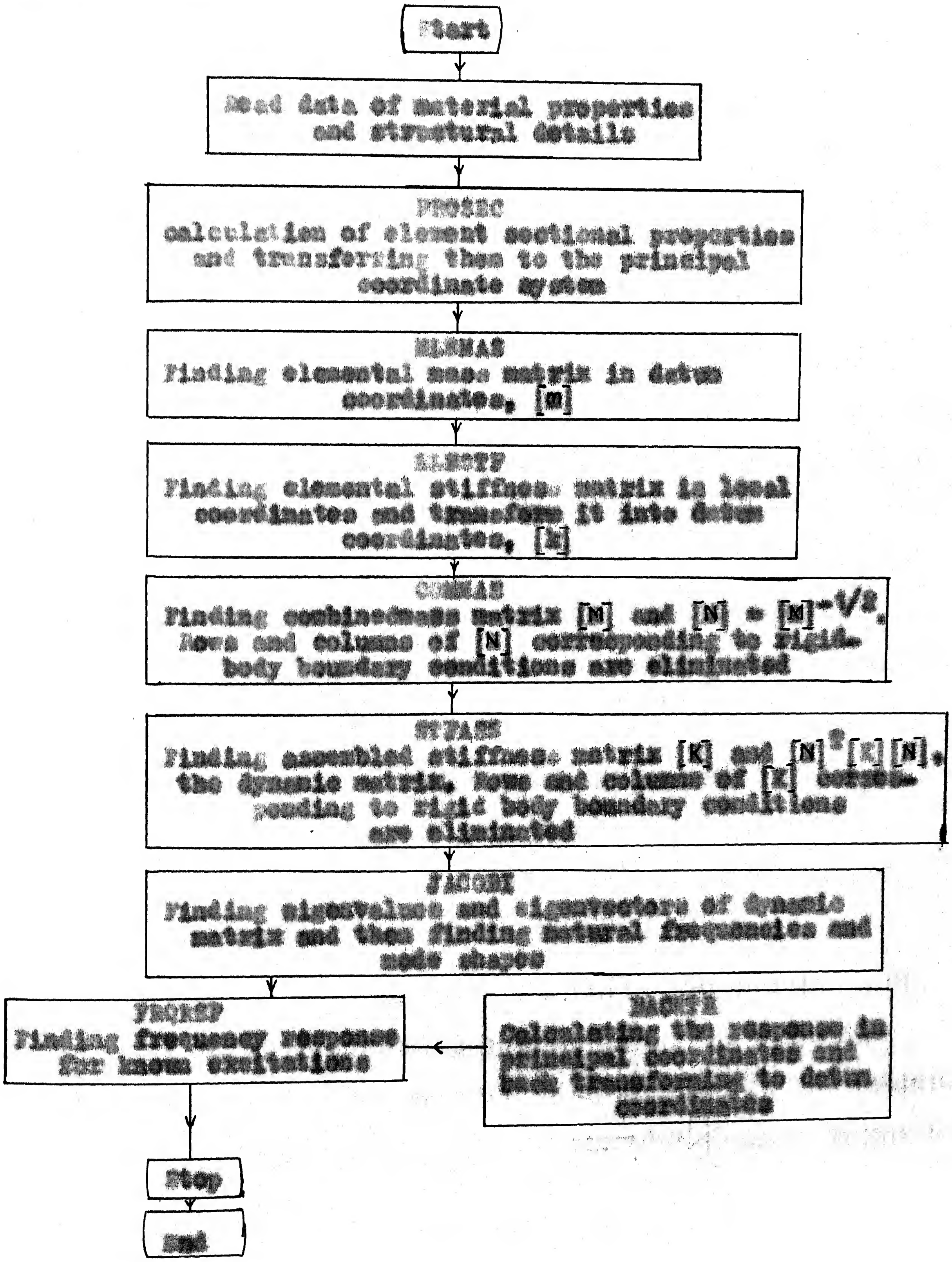

All the sectional properties of elements are evaluated in the subroutine PROSEC.

PROSEC calls in two sub-routines ELEMAS and ELSTF. The elemental mass matrix in the datum coordinates is evaluated in the sub-routine ELEMAS. The matrix being diagonal only the diagonal elements are stored to save memory. The elemental stiffness matrix in the principal coordinates is evaluated in the first part of the subroutine ELSTF and the matrix is transformed into datum coordinates in the second part of ELSTF. The calculations are carried out by storing only the (3x3)$[\Lambda]$ transformation matrix rather than the (12 x 12) $[\lambda]$ matrix.

To evaluate the combined mass matrix, the transformation $[A]^T[\overline{M}][A]$ is replaced by an equivalent summation procedure. In this technique, the elements from $[\overline{M}]_j$ are placed in their correct positions in the larger framework of the matrix $[M]$ and the overlapping terms are added up. This procedure is followed to save time and memory on computer. COMMAS calculates the combined mass matrix $[M]$ and also $[M]^{-1/2}$.

The foregoing summation technique is used to find out the assembled stiffness matrix $[K]$ also. STFASS evaluates $[K]$ and the dynamic matrix $[M]^{-1/2}$ $[K]$ $[M]^{-1/2}$. The dynamic matrix is real, symmetric, and positive-definite.

The eigenvalues and eigenvectors of the dynamic matrix are found out by using Jacobi method. This is an iterative method and it determines accurate eigenvalues and eigenvectors, but poor determination is to be associated with close eigenvalues (See Appendix IV).

Natural frequencies are found out by taking square roots of the corresponding eigenvalues which are obtained in the increasing order of magnitude. Mode shapes, however, are obtained by premultiplying $[M]^{-1/2}$ by the corresponding eigenvectors and normalising them with the maximum component.

Frequency response of the arm is found out in the two sub-routines FRQRSP and BACKTR. FRQRSP calls in BACKTR to determine the response in the principal coordinates and to transform the response back to the datum coordinates.